Summertime fluorescence characteristics of atmospheric water-soluble organic carbon in the marine boundary layer of the western Arctic Ocean

Jinyoung Jung[1], Yuzo Miyazaki[2], Jin Hur[3], Mi Hae Jeon[1], Youngju Lee[1], Kyoung-Ho Cho[1], Hyun Young Chung[1,4], Kitae Kim[1,4], Jung-Ok Choi[1], Catherine Lalande[1], Joo-Hong Kim[1], Taejin Choi[1], Young Jun Yoon[1], Eun Jin Yang[1], and Sung-Ho Kang[1]

[1]Korea Polar Research Institute, 26 Songdomirae-ro, Yeonsu-gu, Incheon 21990, Republic of Korea
[2]Institute of Low Temperature Science, Hokkaido University, Sapporo 060-0819, Japan
[3]Department of Environment & Energy, Sejong University, 209 Neungdong-ro, Gwangjin-gu, Seoul 05006, Republic of Korea
[4]Department of Polar Sciences, University of Science and Technology, Incheon 21990, Republic of Korea

Correspondence to: Jinyoung Jung (jinyoungjung@kopri.re.kr)

Abstract. Accelerated warming and a decline in sea ice coverage in the summertime Arctic Ocean can significantly affect the emissions of marine organic aerosols and biogenic volatile organic compounds. However, how these changes affect the characteristics of atmospheric water-soluble organic carbon (WSOC), which plays an important role in the climate system, remains unclear. Thus, to improve our understanding of WSOC characteristics, including its summertime fluorescence characteristics, in the rapidly changing Arctic Ocean, we simultaneously measured atmospheric concentrations of ionic species and WSOC, fluorescence excitation–emission matrix coupled with parallel factor (EEM–PARAFAC) analysis of WSOC, and marine biological parameters in surface seawaters of the western Arctic Ocean during the summer of 2016. WSOC was predominantly present as fine-mode aerosols (diameter < 2.5 μm) (median = 92 %) with the mean concentration being higher in the coastal water areas (462 ± 130 ngC m^{-3}) than in the sea ice-covered areas (242 ± 88.4 ngC m^{-3}). Moreover, the WSOC in the fine-mode aerosols was positively correlated with the methanesulfonic acid in the fine-mode aerosol samples collected over the sea ice-covered areas (r = 0.88, *p* < 0.01, n = 10), suggesting high sea–air gas exchange and emissions of aerosol precursor gases due to sea ice retreat and increasing available solar radiation during the Arctic summer. Two fluorescent components, humic-like C1 and protein-like C2, were identified by the PARAFAC modeling of fine-mode atmospheric WSOC. The two components varied regionally between coastal and sea ice-covered areas, with low and high fluorescence intensities observed over the coastal areas and sea ice-covered areas, respectively. Further, the humification index of WSOC was correlated with the fluorescence intensity ratio of the humic-like C1/protein-like C2 (r = 0.89, *p* < 0.01) and the WSOC concentration in the fine-mode aerosols (r = 0.66, *p* < 0.05), with the highest values observed in the coastal areas. Additionally, the WSOC concentration in the fine-mode aerosols was positively correlated with the fluorescence intensity ratio of the humic-like C1/protein-like C2 (r = 0.77, *p* < 0.01), but was negatively correlated to the biological index (r = −0.69, *p* < 0.01). Overall, these results suggested that the WSOC in the fine-mode aerosols in the coastal areas showed a higher degree of

polycondensation and higher aromaticity compared that in the sea ice-covered areas, where WSOC in the fine-mode aerosols was associated with relatively new, less oxygenated, and biologically-derived secondary organic components. The findings

35 can improve our understanding of the chemical and biological linkages of WSOC at the ocean–sea ice–atmosphere interface.

1 Introduction

Atmospheric marine aerosols significantly influence the Earth's radiative balance, directly by scattering and absorbing solar radiation, and indirectly by acting as cloud condensation nuclei (CCN) (O'Dowd and De Leeuw, 2007; Quinn and Bates, 2011). The composition and sources of marine organic aerosols are particularly important because organic compounds in aerosols

40 affect the water affinity of aerosols (i.e., hydrophilicity or hydrophobicity) depending on their composition and mixing state, thereby altering CCN formation (Kanakidou et al., 2005). Accordingly, numerous studies have investigated the roles of marine organic aerosols in the climate system, specifically focusing on the characterization and quantification of marine organic aerosols (O'Dowd et al., 2004; Cavalli et al., 2004; Ceburnis et al., 2008; Facchini et al., 2008; Hawkins and Russell, 2010; Russell et al., 2010; Gantt et al., 2011; Miyazaki et al., 2011, 2016; Wilson et al., 2015; Dall'Osto et al., 2017; Jung et al.,

45 2020).

Atmospheric water-soluble organic carbon (WSOC) is a major constituent (approximately 30−60%) of organic carbon (OC) in aerosols in the marine boundary layer (O'Dowd et al., 2004; Facchini et al., 2008; Miyazaki et al., 2016; Jung et al., 2020). The hygroscopicity and CCN activity of aerosols depend on the amount and chemical properties of WSOC in aerosols; thus, WSOC is one of the most important carbon components (Saxena et al., 1995; Matsumoto et al., 1997; Ervens et al., 2005).

50 WSOC comprises highly oxidized species with residual aromatic nuclei and aliphatic chains (Decesari et al., 2001); however, these compounds account for only 10−20% of the total WSOC (Fu et al., 2015). Accordingly, the major composition of WSOC remains chemically unresolved. Most WSOC is currently assumed to be composed of the water-soluble fraction of humic-like substances (HULIS), which are operationally defined as a complex mixture of heterogeneous compounds (Graber and Rudich, 2006). Thus, these discrepancies regarding the chemical composition of atmospheric WSOC hinder our understanding of the

55 role of WSOC in aerosol characteristics.

A fluorescence excitation–emission matrix coupled with parallel factor analysis (EEM–PARAFAC) is commonly used to investigate the optical and structural characteristics of chromophores that are responsible for light absorption and fluorescence by complex organic matter in terrestrial and oceanic systems (Coble, 1996; Coble et al., 1998; Stedmon et al., 2003; Yamashita et al., 2008). EEM–PARAFAC provides useful information regarding not only the chemical compositions and sources but also

60 chemical reactions of atmospheric WSOC (Lee et al., 2013; Fu et al., 2015; Chen et al., 2016; Miyazaki et al., 2018; Tsui and McNeill, 2018; Jung et al., 2020; Tang et al., 2021; Wu et al., 2021). For example, Miyazaki et al. (2018) found that the fluorescence intensity ratios of HULIS and protein-like substances in the sub-micrometer sea spray aerosols were significantly larger than in the bulk surface seawater, indicating that the sea-to-air transfer of marine organic compounds leads to the preferential formation of HULIS in the sea spray aerosols. Although EEM–PARAFAC provides a better understanding of the

65 WSOC characteristics, data on the fluorescence properties of atmospheric WSOC at high latitudes, especially in the rapidly
changing Arctic Ocean, remain sparse.

The Arctic Ocean has been changing remarkably in recent decades. Particularly, the most evident change is the reduction in
the extent of the summer sea ice cover that coincides with an intensive loss of multi-year sea ice (Cavalieri and Parkinson,
2012; Perovich et al., 2020), accompanied by accelerated warming (Ballinger et al., 2020) and upward heat flux from the ocean
70 (Shimada et al., 2006). Further, due to the thinning and decrease in the compactness of sea ice (Perovich et al., 2020), the
Arctic Ocean is highly responsive to wind stress (Kwok et al., 2013), which consequently affects the sea-to-air flux of various
biogenic compounds, including OC. Additionally, the reduced sea ice coverage can significantly increase the seasonal marine
primary production owing to a longer growing season and an expansive open water area (Arrigo and van Dijken, 2011, 2015;
Lewis et al., 2020). As the summertime Arctic aerosols are primarily influenced by local and regional sources, rather than
75 long-range transport from mid-latitude sources (Quinn et al., 2002; Stohl, 2006), these summertime changes in the Arctic
Ocean can significantly affect the emissions of marine organic aerosols, biogenic volatile organic compounds (BVOCs), and
atmospheric chemistry. However, studies on the fluorescence properties of atmospheric WSOC in the Arctic are limited (Fu
et al., 2015; Park et al., 2019a). Therefore, investigating the fluorescence properties of atmospheric WSOC in the summertime
marine Arctic boundary is important to improve our understanding of the chemical and biological linkages of WSOC at the
80 ocean-sea ice-atmosphere interface.

Accordingly, this study aimed to investigate the fluorescence properties of WSOC in aerosols collected over the western Arctic
Ocean during the summer of 2016. Further, in situ chlorophyll-a (Chl-a) and dissolved organic carbon (DOC) concentrations
in surface seawater, and the concentrations of atmospheric ionic species and WSOC were measured to better understand the
fluorescence properties of WSOC. Subsequently, based on the acquired data, the differences in the WSOC characteristics
85 between coastal and sea ice-covered areas were discussed to fill the data gaps and improve further modeling and field
observations.

2 Methods

Aerosol and seawater samples were collected during the ARA07B cruise conducted in the western Arctic Ocean aboard Korean
icebreaker IBR/V *Araon* (Fig. 1). The cruise started from Nome, Alaska, on 5 August 2016, sailed over the Chukchi Sea and
90 western Arctic Ocean for 18 d, and returned to Barrow, Alaska, on 22 August 2016.

2.1 Aerosol data

2.1.1 Aerosol sample collection

The aerosol samples were collected continuously with a sampling flow rate of 1000 L min^{-1} on pre-combusted (at 550 °C for
6 h) quartz filters (25 × 20 cm; QR-100, Sibata Scientific Technology Ltd., Japan) using two high-volume aerosol samplers
95 (HV-1000R, Sibata Scientific Technology Ltd.) placed on the upper deck (20 m a.s.l.) of the ship. Particle size selectors for

particulate matter, PM$_{2.5}$ and PM$_{10}$, were installed on the filters of each aerosol sampler to collect fine-mode (diameter (D) < 2.5 μm) and coarse-mode (2.5 μm < D < 10 μm) aerosols, respectively. To avoid contamination from the ship's exhaust, a wind-sector controller was used during the cruise. The wind-sector controller was configured to collect marine aerosol samples only when the relative wind directions were within ±100°, relative to the ship's bow and when the relative wind speeds were

100   > 1 m s^{-1} (Jung et al., 2020). The total sampling time was 1−2 d, during which the total sampling volume was 580−1800 m^3. In total, 13 aerosol samples were collected during the cruise. After sampling, the filters were frozen at −24 °C before further chemical analysis. Meteorological variables (e.g., wind speed, wind direction, air temperature, relative humidity, and solar radiation) were also continuously monitored by a weather monitoring system equipped on the research vessel.

2.1.2 Chemical analysis of ionic species

105   Aerosol samples were analyzed for major ionic species using the method described by Jung et al. (2019, 2020). Briefly, the collected aerosol samples were divided into four equivalent subsamples. Subsequently, one quarter of each sample was extracted with 50 mL Milli-Q water (> 18 MΩ cm^{-1}, Millipore Co.) using an ultrasonic bath for 30 min. The extraction solution was then filtered through a 13 mm diameter, 0.45 μm pore size membrane filter (polytetrafluoroethylene syringe filter, Millipore Co.). The resultant filtrate was analyzed for anions (Cl$^-$, methanesulfonic acid (MSA), NO$_3^-$, and SO$_4^{2-}$) and cations

110   (Na$^+$, NH$_4^+$, K$^+$, Mg^{2+}, and Ca^{2+}) using ion chromatography (ICS-1100, Thermo Scientific Dionex). The instrumental detection limits were: Cl$^-$, 0.05 μg L^{-1}; MSA, 0.02 μg L^{-1}; NO$_3^-$, 0.02 μg L^{-1}; SO$_4^{2-}$, 0.02 μg L^{-1}; Na$^+$, 0.02 μg L^{-1}; NH$_4^+$, 0.14 μg L^{-1}; K$^+$, 0.16 μg L^{-1}; Mg^{2+}, 0.08 μg L^{-1}; and Ca^{2+}, 0.20 μg L^{-1}. Based on the replicate injections, the analytical precision was estimated to be < 5%. Further, assuming that all sodium ions (Na$^+$) in aerosols were derived from sea salt, the non-sea-salt sulfate (nss-SO$_4^{2-}$) concentration was calculated as the difference between the total SO$_4^{2-}$ concentration and the sodium (Na$^+$)

115   concentration multiplied by 0.2516, which represents the SO$_4^{2-}$/Na$^+$ mass ratio in bulk seawater (Millero and Sohn, 1992).

2.1.3 Chemical analysis of water-soluble organic carbon

The other one subsample was ultrasonically extracted with Milli-Q water and then filtered through a syringe filter as described in Sect. 2.1.2. The resultant filtrates were analyzed for total dissolved organic carbon (TDOC) using a total organic carbon (TOC) analyzer (model TOC-L, Shimadzu Inc., Japan). In the analytical system, inorganic carbon was removed by acidifying

120   the samples to pH 2 using 2 M HCl and subsequent sparging for 8 min before conducting the TDOC analysis. Thus, in this study, the TDOC in the filtrates was defined as WSOC (Jung et al., 2020). Milli-Q water and consensus reference material (42−45 μM C for dissolved organic carbon (DOC); deep Florida Strait water obtained from the University of Miami) were measured at every sixth analysis to check the measurement accuracy. Further, the relative standard deviation of the WSOC analysis for the reproducibility test (at least three measurements per sample) was < 3%.

125   2.1.4 Fluorescence measurement of atmospheric WSOC

The other one subsample was ultrasonically extracted using the same measurement method as that used for ionic species.

Three-dimensional fluorescence EEMs were measured using a luminescence spectrometer (Hitachi F-7000, Hitachi Inc., Japan) at the excitation−emission (Ex−Em) wavelengths of 250−500 and 280−550 nm, respectively (Jung et al., 2020). The Ex and Em scans were set at 5 and 1 nm steps, respectively. The inner filter was corrected using absorbance spectrum measured using

130 an ultraviolet-visible spectrophotometer (Shimadzu 1800, Shimadzu Inc., Japan) according to McKnight et al. (2001). Procedures for EEM measurement and Raman unit (RU) normalization are available in previous studies (Lawaetz and Stedmon, 2009; Chen et al., 2018). Further, PARAFAC modeling was performed using MATLAB 7.0.4 with the DOMFluor toolbox. The number of fluorescent components was determined based on split-half validation. The humification index (HIX, ratio of emission intensity 435−480 nm/300−345 nm at 255 nm excitation; Zsolnay et al., 1999), biological index (BIX, ratio of

135 emission intensity 380 nm/430 nm at 310 nm excitation; Huguet et al., 2009), and fluorescence index (FI, ratio of emission intensity 450 nm/500 nm at 370 nm excitation; McKnight et al., 2001) were calculated from the EEMs.

2.2 Sampling and analysis of surface seawater

Surface seawater samples were collected at 31 stations in the Chukchi Sea and western Arctic Ocean to investigate the link between atmospheric WSOC and DOC and Chl-a using a conductivity–temperature–depth and rosette system holding 24 10-

140 L Niskin bottles (SeaBird Electronics, SBE 911 plus) (Fig. 1).

2.2.1 Dissolved organic carbon

Seawater samples for DOC measurements were collected in the Niskin bottles using gravity filtration through an inline pre-combusted (550 °C for 6 h) Whatman GF/F filter held in an acid-cleaned (0.1 M HCl) polycarbonate 47 mm filter holder (PP-47, ADVANTEC) (Jung et al., 2020, 2021). The resultant filtrate was collected in an acid-cleaned glass bottle and subsequently,

145 distributed into two pre-combusted 20 mL glass ampoules using a sterilized serological pipette. Each ampoule was sealed using a torch, quick-frozen, and preserved at −24 °C until further laboratory analysis. Similar to TDOC, DOC was measured using a Shimadzu TOC-L analyzer using the same method. Analytical errors based on the standard deviations for replicated measurements (at least three measurements per sample) were within 5% for DOC (Jung et al., 2021).

2.2.2 In situ chlorophyll-a analysis

150 To analyze Chl-a, seawater samples were filtered through 47 mm GF/F filters, and then extracted with 90% acetone for 24 h. A fluorometer (Trilogy, Turner Designs, USA) was used to measure Chl-a (Lee et al., 2019).

2.3 Backward trajectory analysis

Seven-day backward trajectories were calculated for air masses starting from each aerosol sampling station at altitudes of 500, 1000, and 1500 m above ground level. The Hybrid Single-Particle Lagrangian Integrated Trajectories (HY-SPLIT) model

155 (http://www.ready.noaa.gov/HYSPLIT_traj.php) (Stein et al., 2015) with meteorological input from the National Oceanic and

Atmospheric Administration (NOAA) Global Data Assimilation System (GDAS) database was used to analyze the backward trajectories.

3 Results and discussion

3.1 Major ionic species

160 ### 3.1.1 Sodium (Na⁺)

The concentration of Na^+, an indicator of sea salt aerosol, was 98–820 ng m^{-3}, with 61% (median value for all data) of Na^+ in the coarse-mode aerosols (Fig. 2a). Generally, wind speed significantly influences the effective production flux of sea salt aerosols in the marine boundary layer (de Leeuw et al., 2011). However, Na^+ concentrations were relatively lower than the mean wind speed (samples AR4−AR8) in sea ice-covered areas, suggesting that the emission of sea salt aerosols by local wind

165 was hindered by sea ice coverage due to decreased wind fetch in the sea ice-covered areas (Nilsson et al., 2001; Held et al., 2011). Additionally, several sea fog events occurred (i.e., air temperature dropped to the dew point, and relative humidity was close to 100%) during the sampling period, and the AR1, AR3, AR4, AR6, AR8, and AR9 aerosol samples were largely or slightly affected by these sea fog events (Fig. 3). Previous studies (Jacob et al., 1984; Bergin et al., 1995; Sasakawa et al., 2003; Herckes et al., 2007; Jung et al., 2013, 2019) demonstrated that compared with fine aerosols, coarse aerosols (D > 0.5

170 μm) predominantly acted as condensation nuclei of sea fog droplets, and that the water vapor condensation on pre-existing particles increases the aerosol size and accelerates their removal from the atmosphere. Similarly, in this study, Na^+ concentration in the coarse-mode aerosols was not correlated with mean wind speed (r = 0.35, p > 0.2), whereas Na^+ concentration in the fine-mode aerosols was significantly correlated with the mean wind speed (r = 0.68, p < 0.05). The absence of correlation between the Na^+ concentration in the coarse-mode aerosols and mean wind speed implied a lower flux of sea

175 salt aerosols relative to the wind speed in sea ice-covered conditions and/or the preferential removal of Na^+ in the coarse-mode aerosols by sea fog.

3.1.2 Nitrate (NO₃⁻)

The NO_3^- concentration ranged from 5.3 to 298 ng m^{-3}, with an average of 44 ± 84 ng m^{-3} (Fig. 2b). Similar to prior observations (Leck and Persson, 1996; Hara et al., 1999; Beine et al., 2003; Kawamura et al., 2007), NO_3^- was mainly

180 associated with the coarse-mode aerosols (median = 65%) because gaseous nitric acid derived from nitrogen oxides (NO_x) emissions was adsorbed on sea-salt aerosols in the marine atmosphere (Andreae and Crutzen, 1997). Among all aerosol samples collected from the coastal areas (AR1−AR3), AR1 exhibited the lowest NO_3^- concentration (42 ng m^{-3}), although the sampling was conducted close to Alaska and Russia (Fig. 1). As NO_3^- was mainly present in the coarse-mode aerosols, the lowest NO_3^- concentration in the coastal areas was attributed to efficient scavenging of coarse aerosols by sea fog, as mentioned

185 previously. When air masses originating from the subarctic western North Pacific Ocean moved over Alaska and thereafter

reached the sampling locations of AR2 and AR3, the NO_3^- concentrations in the coastal areas sharply increased from 42 ng m^{-3} to 298 ng m^{-3} (Fig. 4). However, the concentrations drastically decreased when the samples were collected from the sea ice-covered areas of the western Arctic Ocean, with values reaching constant values of 10 ± 4.9 ng m^{-3}. A similar decreasing trend of NO_3^- concentration with increasing latitude in the Arctic Ocean was also observed by Yu et al. (2020), suggesting that higher NO_3^- concentrations in AR1−AR3 were most likely affected by strong continental sources than those in other samples (Hole et al., 2009). In addition to continental sources, NO_x can be released in the Arctic by the photochemical loss of NO_3^- in the snowpack through the interaction of UV light with snow surfaces. Moreover, the concomitant oxidation of NO_x by bromine oxide could be an important source of NO_3^-, as solar radiation increases during spring and summer (Grannas et al., 2007; Morin et al., 2008). Atmospheric circulation during summer is also confined within the Arctic region (Stohl, 2006; Nielsen et al., 2019), and the backward trajectory analyses showed that air masses circulated over the Arctic Ocean when the sea ice-covered areas were observed (Fig. 4). Therefore, NO_3^- concentrations determined from the sea ice-covered areas were less likely affected by continental sources and were instead derived from local sources.

3.1.3 Methanesulfonic acid (MSA)

The concentration of MSA, a tracer for dimethylsulfide (DMS) input to aerosols, was 10−188 ng m^{-3}, with an average of 72 ± 56 ng m^{-3} (Fig. 2c). Although the mean MSA concentration was 6.5 times higher than that observed at Barrow in August (11 ± 10 ng m^{-3}; Quinn et al., 2002), it was within the MSA concentration ranges previously observed in the Arctic marine boundary layer (e.g., Leck and Persson, 1996; Kerminen and Leck, 2001). MSA was predominantly associated with the fine-mode aerosols (median = 80 %). Further, the MSA concentrations were higher in the sea ice-covered areas than in the coastal areas of the southern Chukchi Sea, whereas in situ surface Chl-a concentrations were high in the southern Chukchi Sea (Fig. S1). Temperature-dependent oxidation pathways of atmospheric DMS (i.e., high MSA yield at low temperatures) can possibly explain the high MSA concentrations at high latitudes (Hynes et al., 1986; Ayers et al., 1991; Bates et al., 1992; Jung et al., 2014, 2020). Indeed, a gradual increase in the MSA concentration from AR1 to AR3 during the sampling periods coincided with a decrease in the air temperature (Figs. 2c and 3). Moreover, the release of DMS, which is produced by whether ice algae and phytoplankton or trapped under the ice or in melt ponds during sea ice retreat or melt, can be attributed to high MSA concentrations in the sea ice-covered areas (Levasseur, 2013; Park et al., 2019b).

3.1.4 Non-sea-salt sulfate (nss-SO$_4^{2-}$)

The nss-SO$_4^{2-}$ concentration was 178–421 ng m^{-3}, with an average of 285 ± 71 ng m^{-3} (Fig. 2d) and approximately 88% (median value) present in the fine-mode aerosols. Unlike NO_3^-, nss-SO$_4^{2-}$ did not show a strong latitudinal gradient, most likely due to the influences of both continental (e.g., fossil fuel combustion and sulfide ore smelting) and marine biogenic (i.e., oxidation of atmospheric DMS from oceanic biological processes) sources (Quinn et al., 2002; Ghahremaninezhad et al., 2016; Nielsen et al., 2019). The mean nss-SO$_4^{2-}$ concentration was approximately 3.5 times lower than that measured at Alert during spring (820−1000 ng m^{-3}, mean = 990 ng m^{-3}; Narukawa et al., 2008), but was 3.2 times higher than that observed at Barrow

in August (90 ± 60 ng m^{-3}; Quinn et al., 2002). These results indicated a strong seasonal variation in nss-SO$_4{}^{2-}$, with minimum and maximum values observed in summer and winter, respectively (e.g., Quinn et al., 2002, 2007; Leaitch et al., 2018) (see

220 Sect. 3.2 for details). Compared with the previous observation at Barrow (Quinn et al., 2002), the mean nss-SO$_4{}^{2-}$ concentration was higher in this study possibly because of an apparent influence of marine biogenic sources in the western Arctic Ocean during summer when anthropogenic nss-SO$_4{}^{2-}$ concentrations are expected to be lower (Quinn et al., 2002). This was supported by the correlation observed between nss-SO$_4{}^{2-}$ and MSA in the fine-mode aerosols ($r = 0.57$, $p < 0.05$, $n = 13$) (Fig. S2a). Moreover, the correlation coefficient increased slightly from 0.57 to 0.65 when only the aerosols collected over the sea ice-

225 covered areas of the western Arctic Ocean (i.e., samples AR4−AR13) were considered ($r = 0.65$, $p < 0.05$, $n = 10$); however, the marginal change in the correlation coefficient was not statistically strong (Fig. S2b). Furthermore, the mean MSA/nss-SO$_4{}^{2-}$ ratio in the fine-mode aerosols (0.21 ± 0.16) was comparable to the other summertime values measured in the central Arctic Ocean during IAOE-91 (0.22, Leck and Persson, 1996) and ASCOS (0.25 ± 0.02, Chang et al., 2011). This supported the apparent influence of marine sources and although the influence of continental sources was minimal in the sea ice-covered

230 areas of the western Arctic Ocean during the cruise (Fig. 4), it cannot be excluded.

3.2 Atmospheric WSOC concentration

The atmospheric WSOC concentration in bulk (fine + coarse) aerosols during the cruise was 141–656 ngC m^{-3}, with an average of 316 ± 141 ngC m^{-3} (Fig. 5a). However, the WSOC was predominantly found in the fine-mode aerosols, with the mean WSOC percentage in such aerosols being 92 ± 5.0 % (median = 92 %), which was consistent with the findings of previous

235 studies conducted in other oceanic regions (Cavalli et al., 2004; Jung et al., 2020). Further, the mean WSOC concentration in bulk aerosols in the western Arctic Ocean was approximately 1.8 times lower than the mean concentration of total OC in the total suspended particulate aerosols (0.56 ± 0.84 μgC m^{-3}; range = 0.11−2.93 μgC m^{-3}) in the southern Beaufort Sea in the summer of 2009 (3−25 August) (Fu et al., 2013). However, the mean WSOC concentration was 6.6 times higher than the mean value (47.6 ng m^{-3}, range = 7.3−185 ng m^{-3}) of chemically identified organic compounds (sugar compounds and fatty acids)

240 in the southern Beaufort Sea. This suggested that most marine organic aerosols in the Arctic Ocean were still not identified at a molecular level (Fu et al., 2013). Additionally, the mean WSOC concentration was 1.7 times higher (0.186 μgC m^{-3}, range = 0.041–0.30 μgC m^{-3}) than that observed at Alert in the Canadian High Arctic (Fu et al., 2015), but 1.3 times lower than the average springtime total submicron (PM1) organic mass (OM) concentration (0.41 ± 0.36 μgC m^{-3}) at Barrow (71.5° N, 156.6° W) in 2008 and 2009 (Frossard et al., 2011).

245 Atmospheric OC (or OM) and major ionic species in the Arctic region generally show a strong seasonal variation, with maximum values observed in winter and early spring and minimum concentrations observed in summer, whereas reverse trends were observed for MSA (Sirois and Barrie, 1999; Quinn et al., 2002; Narukawa et al., 2008; Shaw et al., 2010; Fu et al., 2015; Leaitch et al., 2018). This variation can be attributed to the annual cycles of transport pattern, sea ice, temperature, radiation, biological activity, and atmospheric oxidants (Willis et al., 2018 and references therein). Further, the summertime

250 Arctic aerosols were strongly associated with the transport from oceanic regions due to a decreased meridional transport of

atmospheric pollutants from the mid-latitudes to the Arctic (Stohl, 2006). Contrastingly, relatively weak pollutant removal through wet deposition and long-range transport of continental aerosols and their precursors from the mid-latitudes dramatically increase the atmospheric pollutant concentrations in winter and early spring, and this phenomenon is referred to as Arctic Haze (Sirois and Barrie, 1999; Quinn et al., 2002; Stohl, 2006; Quinn et al., 2007, 2009; Leaitch et al., 2013, 2018;

255 Willis et al., 2018). This suggested that marine sources could further contribute to OC (or OM) in late spring and summer. Moreover, marine organic matter contributes to OC in summer through BVOC emissions (Leaitch et al., 2018) and direct sea spray emissions (Russell et al., 2010; Frossard et al., 2011, 2014). As our study was conducted during summer, the observed WSOC concentration would be more influenced by the sea-to-air emission of marine organic matter from the Arctic Ocean. Indeed, the WSOC concentration in the fine-mode aerosols was positively correlated with in situ surface Chl-a ($r = 0.58$, $p <$

260 0.05, Fig. 5b) and surface DOC concentrations ($r = 0.58$, $p < 0.05$, Fig. 5c), indicating that the WSOC concentration was influenced by the sea-to-air emission of marine organic matter produced by biological activities. Although these relationships confirm that the observed WSOC was associated with locally produced marine organic matter, the WSOC concentration was substantially higher than in the Amundsen Sea in West Antarctica (range = 0.070–0.18 µgC m^{-3}, mean = 0.097 ± 0.038 µgC m^{-3}; Jung et al., 2020), where massive phytoplankton blooms are present (Arrigo et al., 2012). This suggested that continental

265 sources may contribute to the WSOC concentration in the western Arctic Ocean, as supported by the variations in the NO_3^- concentrations (Fig. 2b). Moreover, previous studies conducted in summer reported that organic aerosols were influenced by both marine and continental sources in the southeast Beaufort Sea (Fu et al., 2013) and in the central Arctic Ocean (Chang et al., 2011). However, the impact of continental sources on OC remains low during summer (Fu et al., 2013).

3.3 WSOC/Na$^+$ ratio and relationship with in situ surface concentration

270 The OC (or OM)/Na$^+$ ratio in marine aerosols has commonly been used to investigate the organic fraction in sea spray aerosols. Previous studies demonstrated that compared with seawater, the submicron sea spray aerosols produced by bursting of bubbles are enriched in OC (or OM), with an increasing degree of organic enrichment observed with decreasing particle size (O'Dowd et al., 2004; Keene et al., 2007; Facchini et al., 2008; Russell et al., 2010; Frossard et al., 2014; Quinn et al., 2014). Figure 5a shows that the WSOC/Na$^+$ ratios in the fine-mode aerosols (0.49−5.4) were substantially higher than in the coarse-mode

275 aerosols (0.013−1.9). Particularly, the average WSOC/Na$^+$ ratio in the fine-mode aerosols (2.4 ± 1.5) was approximately 6.7 times higher than that in the coarse-mode aerosols (0.36 ± 0.62), which was consistent with previous results, thus, indicating that OC is enriched in submicron sea spray aerosols. However, the WSOC/Na$^+$ ratios of the fine-mode aerosols observed in this study were higher than those measured previously in submicron primary marine aerosol particles having OC/Na$^+$ ranging from 0.1 to 2 (Russell et al., 2010; Frossard et al., 2014). Similarly, Miyazaki et al. (2020) observed higher WSOC/Na$^+$ ratios

280 (0.1−3.4) in the submicron particles collected from Oyashio and its coastal region, suggesting that the ratio is generally larger in the biologically productive oceanic region (e.g., coastal region) than in the non-productive region (e.g., open ocean) (Frossard et al., 2014; Miyazaki et al., 2020). Moreover, WSOC/Na$^+$ ratio and Chl-a concentration can be associated if phytoplankton blooms influenced the WSOC/Na$^+$ ratio in the fine-mode aerosols during the cruise. Indeed, the WSOC/Na$^+$

ratio in the fine-mode aerosols was positively correlated with the surface Chl-a concentrations (r = 0.74, p < 0.01, Fig. S3a),
285   although some aerosol samples (i.e., AR4 and AR5) showed high values even when the surface Chl-a concentrations were low.
In contrast, Quinn et al. (2014) reported high OM fractions in submicron sea spray aerosols collected over both high- and low-chlorophyll oceanic regions, where Chl-a was not correlated with seawater DOC or OM fraction. They also reported that the oceanic source of OC (such as DOC) enriches OC (or OM) in submicron sea spray aerosols, which is uncoupled from local biological activity as measured by Chl-a over large oceanic regions. However, surface Chl-a and surface DOC concentrations
290   were correlated (r = 0.67, p < 0.05, Fig. S3b) in the western Arctic Ocean. This result was consistent with that of previous studies, which reported that surface DOC concentration was generally associated with Chl-a concentration and primary productivity in our study region, especially in the Chukchi Sea (Davis and Benner, 2005; Shen et al., 2012). Overall, the high WSOC/Na$^+$ ratio in the fine-mode aerosols likely resulted from the sea-to-air transfer of the oceanic source of OC partially along with biological productivity.

295   In addition to the influence of phytoplankton blooms, WSOC/Na$^+$ ratios higher than the typical range (0.1−2) can also be because of secondary contributions of photochemical products of primary organic aerosols and/or marine BVOC to the observed aerosols (Frossard et al., 2014; Miyazaki et al., 2016). Moreover, previous studies reported enhanced contributions of secondary organic aerosols in the Arctic regions from late spring to summer (Fu et al., 2009, 2013; Kawamura et al., 2012). Thus, we investigated the relationship between WSOC and MSA (a well-known secondary product of DMS of marine algal
300   origin) in the fine-mode aerosols and found that the two components were poorly correlated when all the samples collected during the cruise were considered (r = 0.087, p > 0.05, n = 13, Fig. 6). This lack of correlation could be likely due to the difference in source strength between WSOC and MSA, such as contributions of continental sources of WSOC and/or temperature-dependent production of MSA, in the coastal areas close to Alaska and Russia (samples AR1−AR3). However, interestingly, WSOC and MSA in the fine-mode aerosols were positively correlated (r = 0.88, p < 0.01, n = 10) in the aerosol
305   samples (AR4−AR13) collected over the sea ice-covered areas (Fig. 6).
Notably, sea ice is inhabited by ice algae and phytoplankton that produces DMS and organic matter, which act as barriers to the sea–air exchange of volatile and semi-volatile organic gases (Levasseur, 2013; Willis et al., 2018; Abbatt et al., 2019; Lannuzel et al., 2020). Recent evidence also shows that organic gases can be released to the atmosphere from snow or sea ice by photochemical processes of organic species derived from biological production, atmospheric deposition, or in situ chemical
310   formation within snow and sea ice (Grannas et al., 2007; McNeill et al., 2012). Thus, sea ice retreat, increasing available solar radiation, and increasing temperatures during the Arctic summer could increase the sea–air gas exchange and emissions of aerosol precursor gases, such as DMS and VOCs, and increase the emission of primary marine aerosols from open water, marginal sea ice zones, and open leads through wind-driven and photochemical processes (Grannas et al., 2007; McNeill et al., 2012; Levasseur, 2013; Mungall et al., 2017; Abbatt et al., 2019). Given the aforementioned possible processes in the sea
315   ice-covered areas in summer along with the appearance of sea fog events (Sect. 3.1.1; Fig. 3), the significant correlation observed between WSOC and MSA in the fine-mode aerosols collected over the sea ice-covered areas was as expected. Thus, the WSOC/Na$^+$ ratio, which was higher than the typical range (0.1−2), and the significant correlation between WSOC and

MSA in the fine-mode aerosols suggested a strong association of WSOC with secondary processes, such as the condensation of VOCs and related oxidation products on pre-existing sea spray aerosols and the chemical transformation of primary components in the condensed phase (Rinaldi et al., 2010), at least in the sea ice-covered areas.

3.4 Fluorescence properties of water-soluble organic carbon

Two components were identified by the PARAFAC analysis (Fig. 7). Component 1 (C1) shows primary and secondary excitation peaks around 230 nm and 295 nm, respectively, and a single emission peak around 410 nm, which is defined as a mixture of Peaks A and M (terrestrial and marine humic-like fluorescence signals, respectively) (Coble, 1996; Ishii and Boyer, 2012). The spectral features of Peak A are derivatives of terrestrial organic material from river runoff, while components similar to Peak M represent dissolved organic matter (DOM) of biological and microbial origin (Coble et al., 1998; Yamashita et al., 2013; Gao and Guéguen, 2017). The humic-like component, corresponding to C1 in this study, has been previously found in oceanic regions influenced by river runoff (Yamashita et al., 2008, 2011; Fellman et al., 2010). Similarly, other studies have identified this humic-like component in the Arctic Ocean (Gao and Guéguen, 2017; Brogi et al., 2019) due to a strong influence of terrestrial DOC from Arctic rivers (Holmes et al., 2012; Jung et al., 2021). Component 2 (C2) shows a primary excitation maximum at 225 nm, followed by a secondary peak at 270 nm and an emission maximum at 330 nm, which corresponds to Peak T, is considered as a protein-like (or tryptophan-like) labile component produced from biological production in marine environments (Coble, 1996; Coble et al., 1998; Yamashita and Tanoue, 2008; Dainard et al., 2015; Gonçalves-Araujo et al., 2016).

Humic-like substances in aerosols can originate from primary or secondary sources (Graber and Rudich, 2006). For example, biomass burning (Hoffer et al., 2006), fossil fuel combustion (Fan et al., 2016), and bursting of seawater bubbles (Cavalli et al., 2004; Miyazaki et al., 2018) are major primary sources of humic-like substances in aerosols. Secondary sources include multiphase reactions (e.g., oxidation, condensation, oligomerization, and polymerization) of phenolic and carbonyl compounds, as well as other VOCs from biogenic and anthropogenic sources (Gelencsér et al., 2002, 2003; Graber and Rudich, 2006; Wu et al., 2021 and references therein). The uptake of organic species (e.g., dicarbonyls and dicarboxylic acids) to aqueous aerosols via aqueous-phase oligomerization reactions is another source of secondary organic aerosol materials, which exhibit humic-like characteristics (Graber and Rudich, 2006; Nozière et al., 2007). Additionally, the humic-like substances in polar regions can originate from photochemical processes of biogenic organic species in snow and ice, reemission of natural and anthropogenic aerosols trapped in the snow or previously deposited on sea ice, and in situ chemical formation within snow and sea ice (Cini et al., 1994, 1996; Grannas et al., 2007; Beine et al., 2012; McNeill et al., 2012; Voisin et al., 2012). Protein-like substances in aerosols can originate from primary emissions and secondary processes from both anthropogenic (e.g., biomass burning) and biogenic (e.g., spores, pollen, terrestrial and marine organic compounds) sources (Chen et al., 2016; Dall'Osto et al., 2017; Jung et al., 2020; Wu et al., 2021).

In our study, the fluorescence intensities of humic-like C1 and protein-like C2 differed regionally, with lower values (0.36 ± 0.046 RU for C1 and 0.22 ± 0.028 RU for C2) observed over the coastal areas (samples AR1−AR3) and higher values (0.44 ±

0.045 RU for C1 and 0.48 ± 0.10 RU for C2) observed over the sea ice-covered areas (samples AR4−AR13) (Figs. 8a).

Moreover, the mean contribution of the humic-like C1 in the coastal areas was 62 ± 4.6%, which decreased to 48 ± 5.3% in

the sea ice-covered areas (Fig. 8b). Contrastingly, the protein-like C2 showed an opposite trend, with higher contributions in

the sea ice-covered areas (52 ± 5.3%) and lower contributions in the coastal areas (38 ± 4.6%), despite the mean WSOC

355 concentration in the fine-mode aerosols in the sea ice-covered areas (242 ± 88.4 ngC m^{-3}) being lower than in the coastal areas

(462 ± 130 ngC m^{-3}).

The WSOC concentration in fine-mode aerosols increased with increasing contribution of the humic-like C1 (r = 0.69, p <

0.01), but was negatively correlated with the contribution of the protein-like C2 (r = 0.69, p < 0.01) (Fig. 8b). Moreover, the

WSOC concentration in fine-mode aerosols was positively correlated with the fluorescence intensity ratio of the humic-like

360 C1/protein-like C2 (r = 0.77, p < 0.01) (Fig. 8c). Similar results were found at Alert in the Canadian High Arctic during

February–June by Fu et al. (2015), who observed a decrease in the contribution of WSOC to OC with increasing ratio of

protein-like fluorescence to humic-like fluorescence in the WSOC fraction. Additionally, Fu et al. (2015) reported that the

fluorescence intensity ratio of the protein-like to humic-like components showed positive and negative correlations with the

contributions of water-insoluble organic carbon (WIOC) and WSOC to OC, respectively, which were attributed to enhanced

365 sea-to-air emissions of primary marine organic aerosols (i.e., WIOC) in spring. Moreover, Miyazaki et al. (2018) reported

higher ratios (1.3−2.6) of the humic-like (Peak M)/protein-like (Peak T) fluorescence intensity in sea spray aerosols, with

411−1519 ngC m^{-3} WSOC concentration, than those (0.52−1.5) in surface seawater. They attributed these results to the

preferential partitioning of humic-like compounds in the bubble films that produce sea spray aerosols (Burrows et al., 2014;

Elliott et al., 2014), preferential formation of humic-like compounds in sea spray aerosols by aggregation of the precursor

370 materials of the humic-like compound (Gelencsér et al., 2003; Graber and Rudich, 2006; Laskin et al., 2015), or rapid

production of microbial marine humic-like compounds accompanied by rapid degradation of the protein-like compound by

photochemical and/or microbial activity at the sea surface (Yamashita and Tanoue, 2004).

To elucidate the humic-like C1 properties, we investigated the correlations between the humic-like C1 and the FI, BIX, and

HIX, which have been previously used as proxies for the relative contributions of organic matter derived from terrestrial or

375 microbial sources in atmospheric aerosols and in terrestrial and oceanic samples (Lee et al., 2013; Fu et al., 2015; Chen et al.,

2016; Miyazaki et al., 2018; Jung et al., 2020; Tang et al., 2021; Wu et al., 2021). In general, FI values of 1.4 or less indicate

terrestrially derived organics and high aromaticity, whereas values of 1.9 or higher indicate microbial sources and low

aromaticity (McKnight et al., 2001). Further, the increase in BIX is associated with an increase in the contribution of organics

derived from microbes. High values (> 1) correspond to a predominantly biological or microbial origin of DOM along with

380 the presence of organic matter freshly released into water, whereas low values (< 0.6) correspond to DOM with a relatively

smaller contribution from biological materials (Huguet et al., 2009). HIX represents the degree of humification of organic

matter (Zsolnay et al., 1999). High HIX values (> 10) correspond to strongly humified or aromatic organics, principally of

terrestrial origin, whereas low values (< 4) indicate compounds of autochthonous or microbial origin (Birdwell and Engel,

2010; Fu et al., 2015; Tang et al., 2021). Moreover, high HIX values indicate a higher degree of polycondensation (low H/C

385   ratio) and aromaticity (Zsolnay et al., 1999; Qin et al., 2018). Furthermore, the humic-like C1 fluorescence intensity was
positively correlated with FI (r = 0.77, p < 0.01) and BIX (r = 0.61, p < 0.05), but was not correlated with HIX (Figs. 8d−8f).
Overall, high humic-like C1 fluorescence intensity values were observed over the sea ice-covered areas (samples AR4−AR13)
that corresponded to high FI and BIX values. Conversely, humic-like C1 fluorescence intensity values were low in the coastal
areas, and were associated with low FI and BIX values. These results suggested that most humic-like C1, especially over the
390   sea ice-covered areas, was associated with marine biological (or microbial) sources via air-sea-ice (or snow) interactions.

Notably, the fluorescence parameters (i.e., FI, BIX, and HIX) are influenced by photochemical reactions during aging and
transport; thus, the possible sources of atmospheric WSOC should be interpreted carefully (Lee et al., 2013; Chen et al., 2016;
Wu et al., 2021). For example, Chen et al. (2016) found that the FI and BIX were positively correlated with less-oxygenated
ions ($C_xH_y^+$ and $C_xH_yO_1^+$) and negatively correlated with highly oxygenated ions (CO^+ and CO_2^+) in submicron aerosols
395   collected from urban (Nagoya), forest (Kii Peninsula), and marine environments (tropical Eastern Pacific), implying their
association with the oxidation degree of organics. Additionally, Lee et al. (2013) reported that the average values of FI (1.5 ±
0.4) and BIX (0.6) of secondary organic aerosols increased upon aging of secondary organic aerosols, suggesting that
fluorescent secondary organic aerosols may potentially be mistaken for biological particles through fluorescence-based
detection. Wu et al. (2021) reported that the aging process is probably the main factor influencing the HIX values of
400   atmospheric WSOC, with high and low values observed for aged and fresh aerosols, respectively, since the aging process
increases the aromaticity of organic aerosols (Lee et al., 2013). Consequently, the relatively low FI and BIX values, and high
HIX values observed in the coastal areas may suggest that the humic-like C1 in the coastal areas has relatively high aromaticity
and/or more aged organic aerosols. Comparatively, the correlations of FI and BIX with the humic-like C1 fluorescence
intensity and the low HIX values over the sea ice-covered areas could be because the humic-like C1 over the sea ice-covered
405   areas is more affected by relatively new, less-oxygenated, and/or secondary processes (e.g., condensation of VOCs and related
oxidation products on pre-existing aerosols) rather than the marine biological sources, although the biological effect on the
humic-like C1 cannot be ruled out. This claim can be supported by the strong association of WSOC with secondary processes
over the sea ice-covered areas (i.e., significant correlation between WSOC and MSA in the fine-mode aerosols; Sect. 3.3; Fig.
6).

410   Further investigation on the relationships among fluorescence parameters, fluorescence intensity ratio of the humic-like
C1/protein-like C2, and the WSOC concentration in fine-mode aerosols showed that the HIX values were significantly
correlated with the fluorescence intensity ratio of the humic-like C1/protein-like C2 (r = 0.89, p < 0.01) (Fig. 9a) and WSOC
concentration in the fine-mode aerosols (r = 0.66, p < 0.05) (Fig. 9b). The highest HIX values were observed in aerosol samples
collected from the coastal areas (samples AR1 and AR2). Considering the occurrence of sea fog events (Sect. 3.1.1; Fig. 3),
415   the relatively strong influence of anthropogenic sources (Fig. 2b), high WSOC/Na^+ ratio (Sect. 3.3; Fig. 5a), and relationships
shown in Figs. 8, 9a, and 9b, the WSOC in fine-mode aerosols in the coastal areas exhibits high polycondensation degree (low
H/C ratio) and aromaticity (Zsolnay et al., 1999; Qin et al., 2018). Furthermore, the FI value decreased with increasing WSOC
concentration in the fine-mode aerosols, but showed no statistically significant correlation (Fig. 9c). However, the WSOC

concentration in fine-mode aerosols was negatively correlated with the BIX value (r = −0.69, $p < 0.01$) (Fig. 9d). This indicated
420   that the WSOC in the fine-mode aerosols was more likely associated with relatively new, less-oxygenated, and biologically-
derived secondary organic components in the sea ice-covered areas than in the coastal areas (Lee et al., 2013; Chen et al.,
2016).

This study also has some limitations. Our results were obtained over a short sampling period. Moreover, the hydrographic
properties of the Arctic Ocean are radically changing (Ardyna and Arrigo, 2020), which can influence the productions of
425   primary aerosols and secondary aerosol precursors (Lannuzel et al., 2020). Therefore, further studies are required to understand
the characteristics of atmospheric OC more clearly. Additionally, long-term monitoring of atmospheric OC species in the
rapidly changing Arctic Ocean should be conducted.

4 Conclusions

In this study, we reported the summertime fluorescence properties and other WSOC characteristics in marine aerosols collected
430   over the western Arctic Ocean in 2016. Atmospheric concentrations of ionic species and WSOC, EEM spectra of WSOC, and
marine biological parameters in surface seawater were measured simultaneously. This provided better understanding of the
atmospheric WSOC characteristics in the western Arctic Ocean during summer. One such characteristic was a strong
connection of WSOC with secondary processes in the sea ice-covered areas, probably due to greater sea–air gas exchange and
DMS and VOC emissions because of sea ice retreat and increasing available solar radiation during the Arctic summer.
435   The humic-like C1 and protein-like C2 identified by the EEM–PARAFAC analysis of atmospheric WSOC in the fine-mode
aerosols showed that the fluorescence intensities differed regionally between coastal (low intensities) and sea ice-covered areas
(high intensities). Moreover, the relationships between the humic-like C1 and fluorescence parameters (FI, BIX, and HIX)
suggested that the humic-like C1 over the sea ice-covered areas was more likely affected by relatively fresh and/or secondary
processes rather than marine biological sources; however, the biological effect on the humic-like C1 cannot be completely
440   excluded. Additionally, the relationship of the WSOC concentration in fine-mode aerosols with the fluorescence intensity ratio
of the humic-like C1/protein-like C2, HIX, and BIX was studied. The results suggested that the WSOC in the fine-mode
aerosols observed in the coastal areas exhibits higher polycondensation degree (low H/C ratio) and aromaticity than in the sea
ice-covered areas, where the WSOC in fine-mode aerosols was more associated with relatively new, less-oxygenated, and
biologically-derived secondary organic components.
445   Overall, this study enhances our understanding of summertime atmospheric WSOC characteristics over the western Arctic
Ocean.

Data availability

The data used in this study are available on request to the corresponding author Jinyoung Jung (jinyoungjung@kopri.re.kr).

Author contributions

450   JJ designed the research, conducted the experiments, processed the data, and wrote the paper. YM, JH, YL, K-HC, KK, CL, J-HK, TC, and YJY contributed to the scientific discussion and paper correction. EJY and S-HK organized the field campaign and contributed to the scientific discussion and paper correction. MHJ and HYC conducted the experiments. J-OC helped in processing the satellite data.

Competing interests

455   The authors declare that they have no conflict of interest.

Acknowledgements

We thank the captain and crew of the IBR/V *Araon* for their enthusiastic assistance during the ARA07B cruise.

Financial support

This research was a part of the project titled "Korea-Arctic Ocean Warming and Response of Ecosystem (K-AWARE)"
460   supported by the Korea Institute of Marine Science & Technology (KIMST) Promotion grant funded by the Ministry of Oceans and Fisheries, Korea (KIMST 20210605) and by the Korea Polar Research Institute (KOPRI) grant funded by the Ministry of Oceans and Fisheries (KOPRI PE22010).

References

Abbatt, J. P. D., Leaitch, W. R., Aliabadi, A. A., Bertram, A. K., Blanchet, J.-P., Boivin-Rioux, A., Bozem, H., Burkart, J.,
465   Chang, R. Y. W., Charette, J., Chaubey, J. P., Christensen, R. J., Cirisan, A., Collins, D. B., Croft, B., Dionne, J., Evans, G. J., Fletcher, C. G., Galí, M., Ghahremaninezhad, R., Girard, E., Gong, W., Gosselin, M., Gourdal, M., Hanna, S. J., Hayashida, H., Herber, A. B., Hesaraki, S., Hoor, P., Huang, L., Hussherr, R., Irish, V. E., Keita, S. A., Kodros, J. K., Koellner, F., Kolonjari, F., Kunkel, D., Ladino, L. A., Law, K., Levasseur, M., Libois, Q., Liggio, J., Lizotte, M., Macdonald, K. M., Mahmood, R., Martin, R. V., Mason, R. H., Miller, L. A., Moravek, A., Mortenson, E., Mungall, E.
470   L., Murphy, J. G., Namazi, M., Norman, A.-L., O'Neill, N. T., Pierce, J. R., Russell, L. M., Schneider, J., Schulz, H., Sharma, S., Si, M., Staebler, R. M., Steiner, N. S., Thomas, J. L., von Salzen, K., Wentzell, J. J. B., Willis, M. D., Wentworth, G. R., Xu, J.-W., and Yakobi-Hancock, J. D.: Overview paper: New insights into aerosol and climate in the Arctic, Atmos. Chem. Phys., 19, 2527–2560, https://doi.org/10.5194/acp-19-2527-2019, 2019.

Andreae, M. O. and Crutzen, P. J.: Atmospheric aerosols: Biogeochemical sources and role in atmospheric chemistry, Science,
475   276, 1052–1058, https://doi.org/10.1126/science.276.5315.1052, 1997.

Ardyna, M. and Arrigo, K. R.: Phytoplankton dynamics in a changing Arctic Ocean, Nat. Clim. Change, 10, 892–903,

https://doi.org/10.1038/s41558-020-0905-y, 2020.

Arrigo, K. R., Lowry, K. E., and van Dijken, G. L.: Annual changes in sea ice and phytoplankton in polynyas of the Amundsen Sea, Antarctica, Deep-Sea Res., Part II, 71–76, 5–15, https://doi.org/10.1016/j.dsr2.2012.03.006, 2012.

480 Arrigo, K. R. and van Dijken, G. L.: Secular trends in Arctic Ocean net primary production, J. Geophys. Res., 116, C09011, https://doi.org/10.1029/2011JC007151, 2011.

Arrigo, K. R. and van Dijken, G. L.: Continued increases in Arctic Ocean primary production, Prog. Oceanogr., 136, 60–70, https://doi.org/10.1016/j.pocean.2015.05.002, 2015.

Ayers, G. P., Ivey, J. P., and Gillett, R. W.: Coherence between seasonal cycles of dimethyl sulphide, methanesulphonate and

485 sulphate in marine air, Nature, 349, 404–406, https://doi.org/10.1038/349404a0, 1991.

Ballinger, T. J., Overland, J. E., Wang, M., Bhatt, U. S., Hanna, E., Hanssen-Bauer, I., Kim, S. -J., Thomas, R. L., and Walsh, J. E.: Surface air temperature, NOAA Arctic Report Card 2020. https://www.arctic.noaa.gov/Report-Card, 2020.

Bates, T. S., Calhoun, J. A., and Quinn, P. K.: Variations in the methanesulfonate to sulfate molar ratio in submicrometer marine aerosol particles over the South Pacific Ocean, J. Geophys. Res., 97, 9859–9865,

490 https://doi.org/10.1029/92JD00411, 1992.

Beine, H., Anastasio, C., Domine, F., Douglas, T., Barret, M., France, J., King, M., Hall, S., and Ullmann, K.: Soluble chromophores in marine snow, seawater, sea ice and frost flowers near Barrow, Alaska, J. Geophys. Res., 117, D00R15, https://doi.org/10.1029/2011JD016650, 2012.

Beine, H. J., Dominè, F., Ianniello, A., Nardino, M., Allegrini, I., Teinilä, K., and Hillamo, R.: Fluxes of nitrates between snow

495 surfaces and the atmosphere in the European high Arctic, Atmos. Chem. Phys., 3, 335–346, https://doi.org/10.5194/acp-3-335-2003, 2003.

Bergin, M. H., Jaffrezo, J. -L., Davidson, C. I., Dibb, J. E., Pandis, S. N., Hillamo, R., Maenhaut, W., Kuhns, H. D., and Makela, T.: The contributions of snow, fog, and dry deposition to the summer flux of anions and cations at Summit, Greenland, J. Geophys. Res., 100, 16275–16288, https://doi.org/10.1029/95JD01267, 1995.

500 Birdwell, J. E. and Engel, A. S.: Characterization of dissolved organic matter in cave and spring waters using UV–vis absorbance and fluorescence spectroscopy, Org. Geochem., 41, 270–280, https://doi.org/10.1016/j.orggeochem.2009.11.002, 2010.

Brogi, S. R., Jung, J. Y., Ha, S.-Y., and Hur, J.: Seasonal differences in dissolved organic matter properties and sources in an Arctic fjord: Implications for future conditions, Sci. Total Environ., 694, 133740,

505 https://doi.org/10.1016/j.scitotenv.2019.133740, 2019.

Burrows, S. M., Ogunro, O., Frossard, A. A., Russell, L. M., Rasch, P. J., and Elliott, S. M.: A physically based framework for modeling the organic fractionation of sea spray aerosol from bubble film Langmuir equilibria, Atmos. Chem. Phys., 14, 13601–13629, https://doi.org/10.5194/acp-14-13601-2014, 2014.

Cavalieri, D. J. and Parkinson, C. L.: Arctic sea ice variability and trends, 1979–2010, The Cryosphere, 6, 881–889,

510 https://doi.org/10.5194/tc-6-881-2012, 2012.

Cavalli, F., Facchini, M. C., Decesari, S., Mircea, M., Emblico, L., Fuzzi, S., Ceburnis, D., Yoon, Y. J., O'Dowd, C. D., Putaud, J. -P., and Dell'Acqua, A.: Advances in characterization of size-resolved organic matter in marine aerosol over the North Atlantic, J. Geophys. Res., 109, D24215, https://doi.org/10.1029/2004JD005137, 2004.

Ceburnis, D., O'Dowd, C. D., Jennings, G. S., Facchini, M. C., Emblico, L., Decesari, S., Fuzzi, S., and Sakalys, J.: Marine aerosol chemistry gradients: Elucidating primary and secondary processes and fluxes, Geophys. Res. Lett., 35, L07804, https://doi.org/10.1029/2008GL033462, 2008.

Chang, R. Y. W., Leck, C., Graus, M., Müller, M., Paatero, J., Burkhart, J. F., Stohl, A., Orr, L. H., Hayden, K., Li, S. -M., Hansel, A., Tjernström, M., Leaitch, W. R., and Abbatt, J. P. D.: Aerosol composition and sources in the central Arctic Ocean during ASCOS, Atmos. Chem. Phys., 11, 10619–10636, https://doi.org/10.5194/acp-11-10619-2011, 2011.

Chen, M., Jung, J., Lee, Y. K., and Hur, J.: Surface accumulation of low molecular weight dissolved organic matter in surface waters and horizontal off-shelf spreading of nutrients and humic-like fluorescence in the Chukchi Sea of the Arctic Ocean, Sci. Total Environ., 639, 624–632, https://doi.org/10.1016/j.scitotenv.2018.05.205, 2018.

Chen, Q., Miyazaki, Y., Kawamura, K., Matsumoto, K., Coburn, S., Volkamer, R., Iwamoto, Y., Kagami, S., Deng, Y., Ogawa, S., Ramasamy, S., Kato, S., Ida, A., Kajii, Y., and Mochida, M.: Characterization of chromophoric water-soluble organic matter in urban, forest, and marine aerosols by HR-ToF-AMS analysis and excitation–emission matrix spectroscopy, Environ. Sci. Technol., 50, 10351–10360, https://doi.org/10.1021/acs.est.6b01643, 2016.

Cini, R., Innocenti, N. D., Loglio, G., Stortini, A. M., and Tesei, U.: Spectrofluorimetric evidence of the transport of marine organic matter in Antarctic snow via air-sea interaction, Int. J. Environ. Anal. Chem., 55, 285–295, https://doi.org/10.1080/03067319408026226, 1994.

Cini, R., Degliinnocenti, N., Loglio, G., Oppo, C., Orlandi, G., Stortini, A. M., Tesei, U., and Udisti, R.: Air-sea exchange: Sea salt and organic microcomponents in Antarctic Snow, Int. J. Environ. Anal. Chem., 63, 15–27, https://doi.org/10.1080/03067319608039806, 1996.

Coble, P. G.: Characterization of marine and terrestrial DOM in seawater using excitation-emission matrix spectroscopy, Mar. Chem., 51, 325–346, https://doi.org/10.1016/0304-4203(95)00062-3, 1996.

Coble, P. G., Del Castillo, C. E., and Avril, B.: Distribution and optical properties of CDOM in the Arabian Sea during the 1995 Southwest Monsoon, Deep-Sea Res. Part II, 45, 2195–2223, https://doi.org/10.1016/S0967-0645(98)00068-X, 1998.

Dainard, P. G., Guéguen, C., McDonald, N., and Williams, W. J.: Photobleaching of fluorescent dissolved organic matter in Beaufort Sea and North Atlantic Subtropical gyre, Mar. Chem., 177, 630–637, https://doi.org/10.1016/j.marchem.2015.10.004, 2015.

Dall'Osto, M., Ovadnevaite, J., Paglione, M., Beddows, D. C. S., Ceburnis, D., Cree, C., Cortés, P., Zamanillo, M., Nunes, S. O., Pérez, G. L., Ortega-Retuerta, E., Emelianov, M., Vaqué, D., Marrasé, C., Estrada, M., Sala, M. M., Vidal, M., Fitzsimons, M. F., Beale, R., Airs, R., Rinaldi, M., Decesari, S., Facchini, M. C., Harrison, R. M., O'Dowd, C., and Simó, R.: Antarctic sea ice region as a source of biogenic organic nitrogen in aerosols, Sci. Rep., 7, 6047,

545   https://doi.org/10.1038/s41598-017-06188-x, 2017.

Davis, J. and Benner, R.: Seasonal trends in the abundance, composition and bioavailability of particulate and dissolved organic matter in the Chukchi/Beaufort Seas and western Canada Basin, Deep-Sea Res. Part II, 52, 3396–3410, https://doi.org/10.1016/j.dsr2.2005.09.006, 2005.

de Leeuw, G., Andreas, E. L., Anguelova, M. D., Fairall, C. W., Lewis, E. R., O'Dowd, C., Schulz, M., and Schwartz, S. E.:
550   Production flux of sea spray aerosol, Rev. Geophys., 49, RG2001, https://doi.org/10.1029/2010RG000349, 2011.

Decesari, S., Facchini, M. C., Matta, E., Lettini, F., Mircea, M., Fuzzi, S., Tagliavini, E., and Putaud, J. -P.: Chemical features and seasonal variation of fine aerosol water-soluble organic compounds in the Po Valley, Italy, Atmos. Environ., 35, 3691–3699, https://doi.org/10.1016/S1352-2310(00)00509-4, 2001.

Elliott, S., Burrows, S. M., Deal, C., Liu, X., Long, M., Ogunro, O., Russell, L. M., and Wingenter, O.: Prospects for simulating
555   macromolecular surfactant chemistry at the ocean–atmosphere boundary, Environ. Res. Lett., 9, 064012, https://doi.org/10.1088/1748-9326/9/6/064012, 2014.

Ervens, B., Feingold, G., and Kreidenweis, S.: Influence of water-soluble organic carbon on cloud drop number concentration, J. Geophys. Res., 110, D18211, https://doi.org/10.1029/2004JD005634, 2005.

Facchini, M. C., Rinaldi, M., Decesari, S., Carbone, C., Finessi, E., Mircea, M., Fuzzi, S., Ceburnis, D., Flanagan, R., Nilsson,
560   E. D., de Leeuw, G., Martino, M., Woeltjen, J., and O'Dowd, C. D.: Primary submicron marine aerosol dominated by insoluble organic colloids and aggregates, Geophys. Res. Lett., 35, L17814, https://doi.org/10.1029/2008GL034210, 2008.

Fan, X., Wei, S., Zhu, M., Song, J., and Peng, P.: Comprehensive characterization of humic-like substances in smoke $PM_{2.5}$ emitted from the combustion of biomass materials and fossil fuels, Atmos. Chem. Phys., 16, 13321–13340,
565   https://doi.org/10.5194/acp-16-13321-2016, 2016.

Fellman, J. B., Spencer, R. G. M., Hernes, P. J., Edwards, R. T., D'Amore, D. V., and Hood, E.: The impact of glacier runoff on the biodegradability and biochemical composition of terrigenous dissolved organic matter in near-shore marine ecosystems, Mar. Chem., 121, 112–122, https://doi.org/10.1016/j.marchem.2010.03.009, 2010.

Frossard, A. A., Russell, L. M., Burrows, S. M., Elliott, S. M., Bates, T. S., and Quinn, P. K.: Sources and composition of
570   submicron organic mass in marine aerosol particles, J. Geophys. Res.: Atmos., 119, 12977–13003, https://doi.org/10.1002/2014JD021913, 2014.

Frossard, A. A., Shaw, P. M., Russell, L. M., Kroll, J. H., Canagaratna, M. R., Worsnop, D. R., Quinn, P. K., and Bates, T. S.: Springtime Arctic haze contributions of submicron organic particles from European and Asian combustion sources, J. Geophys. Res. Atmos., 116, D05205, https://doi.org/10.1029/2010JD015178, 2011.

575 Fu, P. Q., Kawamura, K., Chen, J., Charrière, B., and Sempéré, R.: Organic molecular composition of marine aerosols over the Arctic Ocean in summer: Contributions of primary emission and secondary aerosol formation, Biogeosciences, 10, 653–667, https://doi.org/10.5194/bg-10-653-2013, 2013.

Fu, P., Kawamura, K., Chen, J., Qin, M., Ren, L., Sun, Y., Wang, Z., Barrie, L. A., Tachibana, E., Ding, A., and Yamashita,

Y.: Fluorescent water-soluble organic aerosols in the High Arctic atmosphere, Sci. Rep., 5, 9845,
580   https://doi.org/10.1038/srep09845, 2015.

Fu, P., Kawamura, K., and Barrie, L. A.: Photochemical and other sources of organic compounds in the Canadian high Arctic
        aerosol pollution during winter-spring, Environ. Sci. Technol., 43, 286–292, https://doi.org/10.1021/es803046q, 2009.

Gantt, B., Meskhidze, N., Facchini, M. C., Rinaldi, M., Ceburnis, D., and O'Dowd, C. D.: Wind speed dependent size-resolved
        parameterization for the organic mass fraction of sea spray aerosol, Atmos. Chem. Phys., 11, 8777–8790,
585   https://doi.org/10.5194/acp-11-8777-2011, 2011.

Gao, Z. and Guéguen, C.: Size distribution of absorbing and fluorescing DOM in Beaufort Sea, Canada Basin, Deep-Sea Res.
        Part I, 121, 30–37, https://doi.org/10.1016/j.dsr.2016.12.014, 2017.

Gelencsér, A., Hoffer, A., Kiss, G., Tombacz, E., Kurdi, R., and Bencze, L.: In-situ formation of light-absorbing organic matter
        in cloud water, J. Atmos. Chem., 45, 25–33, https://doi.org/10.1023/A:1024060428172, 2003.

590   Gelencsér, A., Hoffer, A., Krivacsy, Z., Kiss, G., Molnár, A., and Mészáros, E.: On the possible origin of humic matter in fine
        continental aerosol, J. Geophys. Res., 107, 4137, https://doi.org/10.1029/2001JD001299, 2002.

Ghahremaninezhad, R., Norman, A.-L., Abbatt, J. P. D., Levasseur, M., and Thomas, J. L.: Biogenic, anthropogenic and sea
        salt sulfate size-segregated aerosols in the Arctic summer, Atmos. Chem. Phys., 16, 5191–5202,
        https://doi.org/10.5194/acp-16-5191-2016, 2016.

595   Gonçalves-Araujo, R., Granskog, M. A., Bracher, A., Azetsu-Scott, K., Dodd, P. A., and Stedmon, C. A.: Using fluorescent
        dissolved organic matter to trace and distinguish the origin of Arctic surface waters, Sci. Rep., 6, 33978,
        https://doi.org/10.1038/srep33978, 2016.

Graber, E. R. and Rudich, Y.: Atmospheric HULIS: How humic-like are they? A comprehensive and critical review, Atmos.
        Chem. Phys., 6, 729–753, https://doi.org/10.5194/acp-6-729-2006, 2006.

600   Grannas, A. M., Jones, A. E., Dibb, J., Ammann, M., Anastasio, C., Beine, H. J., Bergin, M., Bottenheim, J., Boxe, C. S.,
        Carver, G., Chen, G., Crawford, J. H., Dominé, F., Frey, M. M., Guzmán, M. I., Heard, D. E., Helmig, D., Hoffmann,
        M. R., Honrath, R. E., Huey, L. G., Hutterli, M., Jacobi, H. W., Klán, P., Lefer, B., McConnell, J., Plane, J., Sander, R.,
        Savarino, J., Shepson, P. B., Simpson, W. R., Sodeau, J. R., von Glasow, R., Weller, R., Wolff, E. W., and Zhu, T.: An
        overview of snow photochemistry: evidence, mechanisms and impacts, Atmos. Chem. Phys., 7, 4329–4373,
605   https://doi.org/10.5194/acp-7-4329-2007, 2007.

Hara, K., Osada, K., Hayashi, M., Matsunaga, K., Shibata, T., Iwasaka, Y., and Furuya, K.: Fractionation of inorganic nitrates
        in winter Arctic troposphere: Coarse aerosol particles containing inorganic nitrates, J. Geophys. Res. Atmos., 104,
        23671–23679, https://doi.org/10.1029/1999JD900348, 1999.

Hawkins, L. N. and Russell, L. M.: Polysaccharides, proteins, and phytoplankton fragments: Four chemically distinct types of
610   marine primary organic aerosol classified by Single Particle spectromicroscopy, Adv. Meteorol., 2010, 1–14,
        https://doi.org/10.1155/2010/612132, 2010.

Held, A., Brooks, I. M., Leck, C., and Tjernström, M.: On the potential contribution of open lead particle emissions to the

central Arctic aerosol concentration, Atmos. Chem. Phys., 11, 3093–3105, https://doi.org/10.5194/acp-11-3093-2011, 2011.

615   Herckes, P., Chang, H., Lee, T., and Collett, J. L., Jr.: Air pollution processing by radiation fogs, Water Air Soil Pollut., 181, 65–75, https://doi.org/10.1007/s11270-006-9276-x, 2007.

Hoffer, A., Gelencsér, A., Guyon, P., Kiss, G., Schmid, O., Frank, G. P., Artaxo, P., and Andreae, M. O.: Optical properties of humic-like substances (HULIS) in biomass-burning aerosols, Atmos. Chem. Phys., 6, 3563–3570, https://doi.org/10.5194/acp-6-3563-2006, 2006.

620   Hole, L. R., Christensen, J. H., Ruoho-Airola, T., Tørseth, K., Ginzburg, V., and Glowacki, P.: Past and future trends in concentrations of sulphur and nitrogen compounds in the Arctic, Atmos. Environ., 43, 928–939, https://doi.org/10.1016/j.atmosenv.2008.10.043, 2009.

Holmes, R. M., McClelland, J. W., Peterson, B. J., Tank, S. E., Bulygina, E., Eglinton, T. I., Gordeev, V. V., Gurtovaya, T. Y., Raymond, P. A., Repeta, D. J., Staples, R., Striegl, R. G., Zhulidov, A. V., and Zimov, S. A.: Seasonal and annual
625   fluxes of nutrients and organic matter from large rivers to the Arctic Ocean and surrounding seas, Estuaries Coasts, 35, 369–382, https://doi.org/10.1007/s12237-011-9386-6, 2012.

Huguet, A., Vacher, L., Relexans, S., Saubusse, S., Froidefond, J. M., and Parlanti, E.: Properties of fluorescent dissolved organic matter in the Gironde Estuary, Org. Geochem., 40(6), 706–719, https://doi.org/10.1016/j.orggeochem.2009.03.002, 2009.

630   Hynes, A. J., Wine, P. H., and Semmes, D. H.: Kinetics and mechanism of hydroxyl reactions with organic sulfides, J. Phys. Chem., 90, 4148–4156, https://doi.org/10.1021/j100408a062, 1986.

Ishii, S. K. L. and Boyer, T. H.: Behavior of reoccurring PARAFAC components in fluorescent dissolved organic matter in natural and engineered systems: A critical review, Environ. Sci. Technol., 46, 2006–2017, https://doi.org/10.1021/es2043504, 2012.

635   Jacob, D. J., Waldman, J. M., Munger, J. W., and Hoffmann, M. R.: A field investigation of physical and chemical mechanisms affecting pollutant concentrations in fog droplets, Tellus B, 36, 272–285, https://doi.org/10.3402/tellusb.v36i4.14909, 1984.

Jung, J., Furutani, H., Uematsu, M., Kim, S., and Yoon, S.: Atmospheric inorganic nitrogen input via dry, wet, and sea fog deposition to the subarctic western North Pacific Ocean, Atmos. Chem. Phys., 13, 411–428, https://doi.org/10.5194/acp-
640   13-411-2013, 2013.

Jung, J., Furutani, H., Uematsu, M., and Park, J.: Distributions of atmospheric non-sea-salt sulfate and methanesulfonic acid over the Pacific Ocean between 48°N and 55°S during summer, Atmos. Environ., 99, 374–384, https://doi.org/10.1016/j.atmosenv.2014.10.009, 2014.

Jung, J., Han, B., Rodriguez, B., Miyazaki, Y., Chung, H. Y., Kim, K., Choi, J.-O., Park, K., Kim, I.-N., Kim, S., Yang, E. J.,
645   and Kang, S.-H.: Atmospheric dry deposition of water-soluble nitrogen to the subarctic western north Pacific Ocean during summer, Atmosphere, 10, 351, https://doi.org/10.3390/atmos10070351, 2019.

Jung, J., Hong, S.-B., Chen, M., Hur, J., Jiao, L., Lee, Y., Park, K., Hahm, D., Choi, J.-O., Yang, E. J., Park, J., Kim, T. W., and Lee, S.: Characteristics of methanesulfonic acid, non-sea-salt sulfate and organic carbon aerosols over the Amundsen Sea, Antarctica, Atmos. Chem. Phys., 20, 5405–5424, https://doi.org/10.5194/acp-20-5405-2020, 2020.

650 Jung, J., Son, J. E., Lee, Y. K., Cho, K.-H., Lee, Y., Yang, E. J., Kang, S.-H., and Hur, J.: Tracing riverine dissolved organic carbon and its transport to the halocline layer in the Chukchi Sea (western Arctic Ocean) using humic-like fluorescence fingerprinting, Sci. Total Environ., 772, 145542, https://doi.org/10.1016/j.scitotenv.2021.145542, 2021.

Kanakidou, M., Seinfeld, J. H., Pandis, S. N., Barnes, I., Dentener, F. J., Facchini, M. C., Van Dingenen, R., Ervens, B., Nenes, A., Nielsen, C. J., Swietlicki, E., Putaud, J. P., Balkanski, Y., Fuzzi, S., Horth, J., Moortgat, G. K., Winterhalter, R., 655 Myhre, C. E. L., Tsigaridis, K., Vignati, E., Stephanou, E. G. and Wilson, J.: Organic aerosol and global climate modelling: a review, Atmos. Chem. Phys., 5, 1053–1123, 2005.

Kawamura, K., Kasukabe, H., and Barrie, L. A.: Source and reaction pathways of dicarboxylic acids, ketoacids and dicarbonyls in Arctic aerosols: One year of observations, Atmos. Environ., 30, 1709–1722, https://doi.org/10.1016/1352-2310(95)00395-9, 1996.

660 Kawamura, K., Narukawa, M., Li, S.-M., and Barrie, L. A.: Size distributions of dicarboxylic acids and inorganic ions in atmospheric aerosols collected during polar sunrise in the Canadian high Arctic, J. Geophys. Res., 112, D10307, https://doi.org/10.1029/2006JD008244, 2007.

Kawamura, K., Ono, K., Tachibana, E., Charriére, B., and Sempéré, R.: Distributions of low molecular weight dicarboxylic acids, ketoacids and α-dicarbonyls in the marine aerosols collected over the Arctic Ocean during late summer, 665 Biogeosciences, 9, 4725–4737, https://doi.org/10.5194/bg-9-4725-2012, 2012.

Keene, W. C., Maring, H., Maben, J. R., Kieber, D. J., Pszenny, A. A. P., Dahl, E. E., Izaguirre, M. A., Davis, A. J., Long, M. S., Zhou, X., Smoydzin, L., and Sander, R.: Chemical and physical characteristics of nascent aerosols produced by bursting bubbles at a model air-sea interface, J. Geophys. Res., 112, D21202, https://doi.org/10.1029/2007JD008464, 2007.

670 Kerminen, V.-M. and Leck, C.: Sulfur chemistry over the central Arctic Ocean during the summer: Gas-to-particle transformation, J. Geophys. Res., 106, 32087–32099, https://doi.org/10.1029/2000JD900604, 2001.

Kwok, R., Spreen, G., and Pang, S.: Arctic sea ice circulation and drift speed: Decadal trends and ocean currents, J. Geophys. Res. Oceans, 118, 2408–2425, https://doi.org/10.1002/jgrc.20191, 2013.

Lannuzel, D., Tedesco, L., van Leeuwe, M., Campbell, K., Flores, H., Delille, B., Miller, L., Stefels, J., Assmy, P., Bowman, 675 J., Brown, K., Castellani, G., Chierici, M., Crabeck, O., Damm, E., Else, B., Fransson, A., Fripiat, F., Geilfus, N.-X., Jacques, C., Jones, E., Kaartokallio, H., Kotovitch, M., Meiners, K., Moreau, S., Nomura, D., Peeken, I., Rintala, J.-M., Steiner, N., Tison, J.-L., Vancoppenolle, M., Van der Linden, F., Vichi, M., and Wongpan, P.: The future of Arctic sea-ice biogeochemistry and ice-associated ecosystems, Nat. Clim. Change, 10, 983–992, https://doi.org/10.1038/s41558-020-00940-4, 2020.

680   Laskin, A., Laskin, J., and Nizkorodov, S. A.: Chemistry of Atmospheric Brown Carbon, Chem. Rev., 115, 4335–4382, https://doi.org/10.1021/cr5006167, 2015.

Lawaetz, A. J. and Stedmon, C. A.: Fluorescence intensity calibration using the Raman scatter peak of water, Appl. Spectrosc., 63, 936–940, https://doi.org/10.1366/000370209788964548, 2009.

Leaitch, W. R., Russell, L. M., Liu, J., Kolonjari, F., Toom, D., Huang, L., Sharma, S., Chivulescu, A., Veber, D., and Zhang,
685   W.: Organic functional groups in the submicron aerosol at 82.5° N, 62.5° W from 2012 to 2014, Atmos. Chem. Phys., 18, 3269–3287, https://doi.org/10.5194/acp-18-3269-2018, 2018.

Leaitch, W. R., Sharma, S., Huang, L., Toom-Sauntry, D., Chivulescu, A., Macdonald, A. M., von Salzen, K., Pierce, J. R., Bertram, A. K., Schroder, J. C., Shantz, N. C., Chang, R. Y. -W., and Norman, A.-L.: Dimethyl sulfide control of the clean   summertime   Arctic   aerosol   and   cloud,   Elem.   Sci.   Anth.,   1:000017,   1–12,
690   https://doi.org/10.12952/journal.elementa.000017, 2013.

Leck, C. and Persson, C.: Seasonal and short-term variability in dimethyl sulfide, sulfur dioxide and biogenic sulfur and sea salt aerosol particles in the arctic marine boundary layer during summer and autumn, Tellus B, 48, 272–299, https://doi.org/10.1034/j.1600-0889.48.issue2.1.x, 1996.

Lee, H. J. J., Laskin, A., Laskin, J., and Nizkorodov, S. A.: Excitation–emission spectra and fluorescence quantum yields for
695   fresh   and   aged   biogenic   secondary   organic   aerosols,   Environ.   Sci.   Technol.,   47,   5763–5770, https://doi.org/10.1021/es400644c, 2013.

Lee, Y., Min, J. O., Yang, E. J., Cho, K.-H., Jung, J., Park, J., Moon, J. K., and Kang, S.-H.: Influence of sea ice concentration on phytoplankton community structure in the Chukchi and East Siberian Seas, Pacific Arctic Ocean, Deep-Sea Res. Part I, 147, 54–64, https://doi.org/10.1016/j.dsr.2019.04.001, 2019.

700   Levasseur, M.: Impact of Arctic meltdown on the microbial cycling of sulphur. Nat. Geosci., 6, 691–700, https://doi.org/10.1038/ngeo1910, 2013.

Lewis, K. M., van Dijken, G. L., and Arrigo, K. R.: Changes in phytoplankton concentration now drive increased Arctic Ocean primary production, Science, 369, 198–202, https://doi.org/10.1126/science.aay8380, 2020.

Matsumoto, K., Tanaka, H., Nagao, I., and Ishizaka, Y.: Contribution of particulate sulfate and organic carbon to cloud
705   condensation nuclei in the marine atmosphere. Geophys. Res. Lett., 24, 655–658, https://doi.org/10.1029/97GL00541, 1997.

McKnight, D. M., Boyer, E. W., Westerhoff, P. K., Doran, P. T., Kulbe, T., and Andersen, D. T.: Spectrofluorometric characterization of dissolved organic matter for indication of precursor organic material and aromaticity, Limnol. Oceanogr., 46, 38–48, https://doi.org/10.4319/lo.2001.46.1.0038, 2001.

710   McNeill, V. F., Grannas, A. M., Abbatt, J. P. D., Ammann, M., Ariya, P., Bartels-Rausch, T., Domine, F., Donaldson, D. J., Guzman, M. I., Heger, D., Kahan, T. F., Klán, P., Masclin, S., Toubin, C., and Voisin, D.: Organics in environmental ices: Sources, chemistry, and impacts, Atmos. Chem. Phys., 12, 9653–9678, https://doi.org/10.5194/acp-12-9653-2012, 2012.

Millero, F. J. and Sohn, M. L.: Chemical oceanography, CRC Press, Boca Raton, FL, 521 pp, 1992.

715   Miyazaki, Y., Coburn, S., Ono, K., Ho, D. T., Pierce, R. B., Kawamura, K., and Volkamer, R.: Contribution of dissolved
            organic matter to submicron water-soluble organic aerosols in the marine boundary layer over the eastern equatorial
            Pacific, Atmos. Chem. Phys., 16, 7695–7707, https://doi.org/10.5194/acp-16-7695-2016, 2016.

Miyazaki, Y., Kawamura, K., Jung, J., Furutani, H., and Uematsu, M.: Latitudinal distributions of organic nitrogen and organic
            carbon in marine aerosols over the western North Pacific, Atmos. Chem. Phys., 11, 3037–3049,
720   https://doi.org/10.5194/acp-11-3037-2011, 2011.

Miyazaki, Y., Suzuki, K., Tachibana, E., Yamashita, Y., Müller, A., Kawana, K., and Nishioka, J.: New index of organic mass
            enrichment in sea spray aerosols linked with senescent status in marine phytoplankton, Sci. Rep., 10, 17042,
            https://doi.org/10.1038/s41598-020-73718-5, 2020.

Miyazaki, Y., Yamashita, Y., Kawana, K., Tachibana, E., Kagami, S., Mochida, M., Suzuki, K., and Nishioka, J.: Chemical
725   transfer of dissolved organic matter from surface seawater to sea spray water-soluble organic aerosol in the marine
            atmosphere, Sci. Rep., 8, 14861, https://doi.org/10.1038/s41598-018-32864-7, 2018.

Morin, S., Savarino, J., Frey, M. M., Yan, N., Bekki, S., Bottenheim, J. W., and Martins, J. M. F.: Tracing the origin and fate
            of NO_x in the Arctic atmosphere using stable isotopes in nitrate, Science, 322, 730–732,
            https://doi.org/10.1126/science.1161910, 2008.

730   Mungall, E. L., Abbatt, J. P. D., Wentzell, J. J. B., Lee, A. K. Y., Thomas, J. L., Blais, M., Gosselin, M., Miller, L. A.,
            Papakyriakou, T., Willis, M. D., and Liggio, J.: Microlayer source of oxygenated volatile organic compounds in the
            summertime marine Arctic boundary layer, Proc. Natl. Acad. Sci. U.S.A., 114, 6203–6208,
            https://doi.org/10.1073/pnas.1620571114, 2017.

Narukawa, M., Kawamura, K., Li, S.-M., and Bottenheim, J. W.: Stable carbon isotopic ratios and ionic composition of the
735   high-Arctic aerosols: An increase in $\delta^{13}C$ values from winter to spring, J. Geophys. Res., 113, D02312,
            https://doi.org/10.1029/2007JD008755, 2008.

Nielsen, I. E., Skov, H., Massling, A., Eriksson, A. C., Dall'Osto, M., Junninen, H., Sarnela, N., Lange, R., Collier, S., Zhang,
            Q., Cappa, C. D., and Nøjgaard, J. K.: Biogenic and anthropogenic sources of Arctic aerosols at the High Arctic site
            Villum Research Station, Atmos. Chem. Phys., 19, 10239–10256, https://doi.org/10.5194/acp-19-10239-2019, 2019.

740   Nilsson, E. D., Rannik, Ü., Swietlicki, E., Leck, C., Aalto, P. P., Zhou, J., and Norman, M.: Turbulent aerosol fluxes over the
            Arctic Ocean: 2. Wind-driven sources from the sea, J. Geophys. Res., 106, 32139–32154,
            https://doi.org/10.1029/2000JD900747, 2001.

Nozière, B., Dziedzic, P., and Córdova, A.: Formation of secondary light-absorbing "fulvic-like" oligomers: A common process
            in aqueous and ionic atmospheric particles? Geophys. Res. Lett., 34, L21812, https://doi.org/10.1029/2007GL031300,
745   2007.

O'Dowd, C. D. and De Leeuw, G.: Marine aerosol production: A review of the current knowledge, Phil. Trans. R. Soc. A, 365,
            1753–1774, https://doi.org/10.1098/rsta.2007.2043, 2007.

O'Dowd, C. D., Facchini, M. C., Cavalli, F., Ceburnis, D., Mircea, M., Decesari, S., Fuzzi, S., Yoon, Y.-J., and Putaud, J.-P.: Biogenically driven organic contribution to marine aerosol, Nature, 431, 676–680, https://doi.org/10.1038/nature02959, 2004.

Park, J., Dall'Osto, M., Park, K., Kim, J.-H., Park, J., Park, K.-T., Hwang, C. Y., Jang, G. I., Gim, Y., Kang, S., Park, S., Jin, Y. K., Yum, S. S., Simó, R., and Yoon, Y.-J.: Arctic primary aerosol production strongly influenced by riverine organic matter, Environ. Sci. Technol., 53, 8621–8630, https://doi.org/10.1021/acs.est.9b03399, 2019a.

Park, K., Kim, I., Choi, J.-O., Lee, Y., Jung, J., Ha, S.-Y., Kim, J.-H., and Zhang, M.: Unexpectedly high dimethyl sulfide concentration in high-latitude Arctic sea ice melt ponds, Environ. Sci.: Processes Impacts, 21, 1642–1649, https://doi.org/10.1039/c9em00195f, 2019b.

Perovich, D., Meier, W., Tschudi, T., Hendricks, S., Petty, A. A., Divine, D., Farrell, S., Gerland, S., Haas, C., Kaleschke, L., Pavlova, O., Ricker, R., Tian-Kunze, X., Webster, M., and Wood, K.: Sea ice, NOAA Arctic Report Card 2020, https://www.arctic.noaa.gov/Report-Card, 2020.

Qin, J., Zhang, L., Zhou, X., Duan, J., Mu, S., Xiao, K., Hu, J., and Tan, J.: Fluorescence fingerprinting properties for exploring water-soluble organic compounds in PM2.5 in an industrial city of northwest China, Atmos. Environ., 184, 203–211, https://doi.org/10.1016/j.atmosenv.2018.04.049, 2018.

Quinn, P. K. and Bates, T. S.: The case against climate regulation via oceanic phytoplankton sulphur emissions, Nature, 480, 51–56, https://doi.org/10.1038/nature10580, 2011.

Quinn, P. K., Bates, T. S., Schulz, K. S., Coffman, D. J., Frossard, A. A., Russell, L. M., Keene, W. C., and Kieber, D. J.: Contribution of sea surface carbon pool to organic matter enrichment in sea spray aerosol, Nat. Geosci., 7, 228–232, https://doi.org/10.1038/NGEO2092, 2014.

Quinn, P. K., Bates, T. S., Schulz, K., and Shaw, G. E.: Decadal trends in aerosol chemical composition at Barrow, Alaska: 1976–2008, Atmos. Chem. Phys., 9, 8883–8888, https://doi.org/10.5194/acp-9-8883-2009, 2009.

Quinn, P. K., Miller, T. L., Bates, T. S., Ogren, J. A., Andrews, E., and Shaw, G. E.: A 3-year record of simultaneously measured aerosol chemical and optical properties at Barrow, Alaska, J. Geophys. Res., 107, AAC 8–1–AAC 8–15, https://doi.org/10.1029/2001JD001248, 2002.

Quinn, P. K., Shaw, G., Andrews, E., Dutton, E. G., Ruoho-Airola, T., and Gong, S. L.: Arctic haze: current trends and knowledge gaps, Tellus B: Chem. Phys. Meteorol., 59(1), 99–114, https://doi.org/10.1111/j.1600-0889.2006.00236.x, 2007.

Rinaldi, M., Decesari, S., Finessi, E., Giulianelli, L., Carbone, C., Fuzzi, S., O'Dowd, C. D., Ceburnis, D., and Facchini, M. C.: Primary and secondary organic marine aerosol and oceanic biological activity: Recent results and new perspectives for future studies, Adv. Meteorol., 2010, 1–10, https://doi.org/10.1155/2010/310682, 2010.

Russell, L. M., Hawkins, L. N., Frossard, A. A., Quinn, P. K., and Bates, T. S.: Carbohydrate-like composition of submicron atmospheric particles and their production from ocean bubble bursting, Proc. Natl. Acad. Sci. U.S.A., 107, 6652–6657, https://doi.org/10.1073/pnas.0908905107, 2010.

Sasakawa, M., Ooki, A., and Uematsu, M.: Aerosol size distribution during sea fog and its scavenge process of chemical substances over the northwestern North Pacific, J. Geophys. Res., 108, 4120, https://doi.org/10.1029/2002JD002329, 2003.

785 Saxena, P., Hildemann, L. M., McMurry, P. H., and Seinfeld, J. H.: Organics alter hygroscopic behavior of atmospheric particles, J. Geophys. Res., 100, 18755–18770, https://doi.org/10.1029/95JD01835, 1995.

Shaw, P. M., Russell, L. M., Jefferson, A., and Quinn, P. K.: Arctic organic aerosol measurements show particles from mixed combustion in spring haze and from frost flowers in winter, Geophys. Res. Lett., 37, L10803, https://doi.org/10.1029/2010GL042831, 2010.

790 Shen, Y., Fichot, C. G., and Benner, R.: Dissolved organic matter composition and bioavailability reflect ecosystem productivity in the Western Arctic Ocean, Biogeosciences, 9, 4993–5005, https://doi.org/10.5194/bg-9-4993-2012, 2012.

Shimada, K., Kamoshida, T., Itoh, M., Nishino, S., Carmack, E., McLaughlin, F., Zimmermann, S., and Proshutinsky, A.: Pacific Ocean inflow: Influence on catastrophic reduction of sea ice cover in the Arctic Ocean, Geophys. Res. Lett., 33, L08605, https://doi.org/10.1029/2005GL025624, 2006.

795 Sirois, A. and Barrie, L. A.: Arctic lower tropospheric aerosol trends and composition at Alert, Canada: 1980−1995, J. Geophys. Res., 104, 11599–11618, https://doi.org/10.1029/1999JD900077, 1999.

Spreen, G., Kaleschke, L., and Heygster, G.: Sea ice remote sensing using AMSR-E 89-GHz channels, J. Geophys. Res., 113, C02S03, https://doi.org/10.1029/2005JC003384, 2008.

Stedmon, C. A., Markager, S., and Bro, R.: Tracing dissolved organic matter in aquatic environments using a new approach to 800 fluorescence spectroscopy, Mar. Chem., 82, 239–254, https://doi.org/10.1016/S0304-4203(03)00072-0, 2003.

Stein, A. F., Draxler, R. R., Rolph, G. D., Stunder, B. J. B, Cohen, M. D., and Ngan, F.: NOAA's HYSPLIT atmospheric transport and dispersion modeling system. Bull. Amer. Meteorol. Soc., 96, 2059–2077, http://dx.doi.org/10.1175/BAMS-D-14-00110.1, 2015.

Stohl, A.: Characteristics of atmospheric transport into the Arctic troposphere, J. Geophys. Res., 111, D11306, 805 https://doi.org/10.1029/2005JD006888, 2006.

Tang, J., Wang, J., Zhong, G., Jiang, H., Mo, Y., Zhang, B., Geng, X., Chen, Y., Tang, J., Tian, C., Bualert, S., Li, J., and Zhang, G.: Measurement report: Long-emission-wavelength chromophores dominate the light absorption of brown carbon in aerosols over Bangkok: impact from biomass burning, Atmos. Chem. Phys., 21, 11337–11352, https://doi.org/10.5194/acp-21-11337-2021, 2021.

810 Tsui, W. G. and McNeill, V. F.: Modeling secondary organic aerosol production from photosensitized humic-like substances (HULIS), Environ. Sci. Technol. Lett., 5, 255–259, https://doi.org/10.1021/acs.estlett.8b00101, 2018.

Voisin, D., Jaffrezo, J.-L., Houdier, S., Barret, M., Cozic, J., King, M. D., France, J. L., Reay, H. J., Grannas, A., Kos, G., Ariya, P. A., Beine, H. J., and Domine, F.: Carbonaceous species and humic like substances (HULIS) in Arctic snowpack during OASIS field campaign in Barrow, J. Geophys. Res., 117, D00R19, https://doi.org/10.1029/2011JD016612, 2012.

815 Willis, M. D., Leaitch, W. R., and Abbatt, J. P. D.: Processes controlling the composition and abundance of Arctic aerosol, Rev.

Geophys., 56, 621–671, https://doi.org/10.1029/2018RG000602, 2018.

Wilson, T. W., Ladino, L. A., Alpert, P. A., Breckels, M. N., Brooks, I. M., Browse, J., Burrows, S. M., Carslaw, K. S., Huffman, J. A., Judd, C., Kilthau, W. P., Mason, R. H., McFiggans, G., Miller, L. A., Nájera, J. J., Polishchuk, E., Rae, S., Schiller, C. L., Si, M., Temprado, J. V., Whale, T. F., Wong, J. P. S., Wurl, O., Yakobi-Hancock, J. D., Abbatt, J. P. D., Aller, J. Y.,

820   Bertram, A. K., Knopf, D. A., and Murray, B. J.: A marine biogenic source of atmospheric ice-nucleating particles, Nature, 525, 234–238, https://doi.org/10.1038/nature14986, 2015.

Wu, G., Fu, P., Ram, K., Song, J., Chen, Q., Kawamura, K., Wan, X., Kang, S., Wang, X., Laskin, A., and Cong, Z.: Fluorescence characteristics of water-soluble organic carbon in atmospheric aerosol, Environ. Pollut., 268, 115906, https://doi.org/10.1016/j.envpol.2020.115906, 2021.

825 Yamashita, Y., Boyer, J. N., and Jaffé, R.: Evaluating the distribution of terrestrial dissolved organic matter in a complex coastal ecosystem using fluorescence spectroscopy, Con. Shelf Res., 66, 136–144, https://doi.org/10.1016/j.csr.2013.06.010, 2013.

Yamashita, Y., Jaffé, R., Maie, N., and Tanoue, E.: Assessing the dynamics of dissolved organic matter (DOM) in coastal environments by excitation emission matrix fluorescence and parallel factor analysis (EEM-PARAFAC), Limnol.

830   Oceanogr., 53, 1900–1908, https://doi.org/10.4319/lo.2008.53.5.1900, 2008.

Yamashita, Y., Panton, A., Mahaffey, C., and Jaffé, R.: Assessing the spatial and temporal variability of dissolved organic matter in Liverpool Bay using excitation–emission matrix fluorescence and parallel factor analysis, Ocean Dyn., 61, 569–579, https://doi.org/10.1007/s10236-010-0365-4, 2011.

Yamashita, Y. and Tanoue, E.: In situ production of chromophoric dissolved organic matter in coastal environments, Geophys.

835   Res. Lett., 31, L14302, https://doi.org/10.1029/2004GL019734, 2004.

Yamashita, Y. and Tanoue, E.: Production of bio-refractory fluorescent dissolved organic matter in the ocean interior, Nat. Geosci., 1, 579–582, https://doi.org/10.1038/ngeo279, 2008.

Yu, C., Yan, J., Zhang, H., Lin, Q., Zheng, H., Zhong, X., Zhao, S., Zhang, M., Zhao, S., and Li, X.: Characteristics of aerosol WSI with high-time-resolution observation over Arctic Ocean, Earth Space Sci., 7, e2020EA001227,

840   https://doi.org/10.1029/2020EA001227, 2020.

Zsolnay, A., Baigar, E., Jimenez, M., Steinweg, B., and Saccomandi, F.: Differentiating with fluorescence spectroscopy the sources of dissolved organic matter in soils subjected to drying, Chemosphere, 38, 45–50, https://doi.org/10.1016/S0045-6535(98)00166-0, 1999.
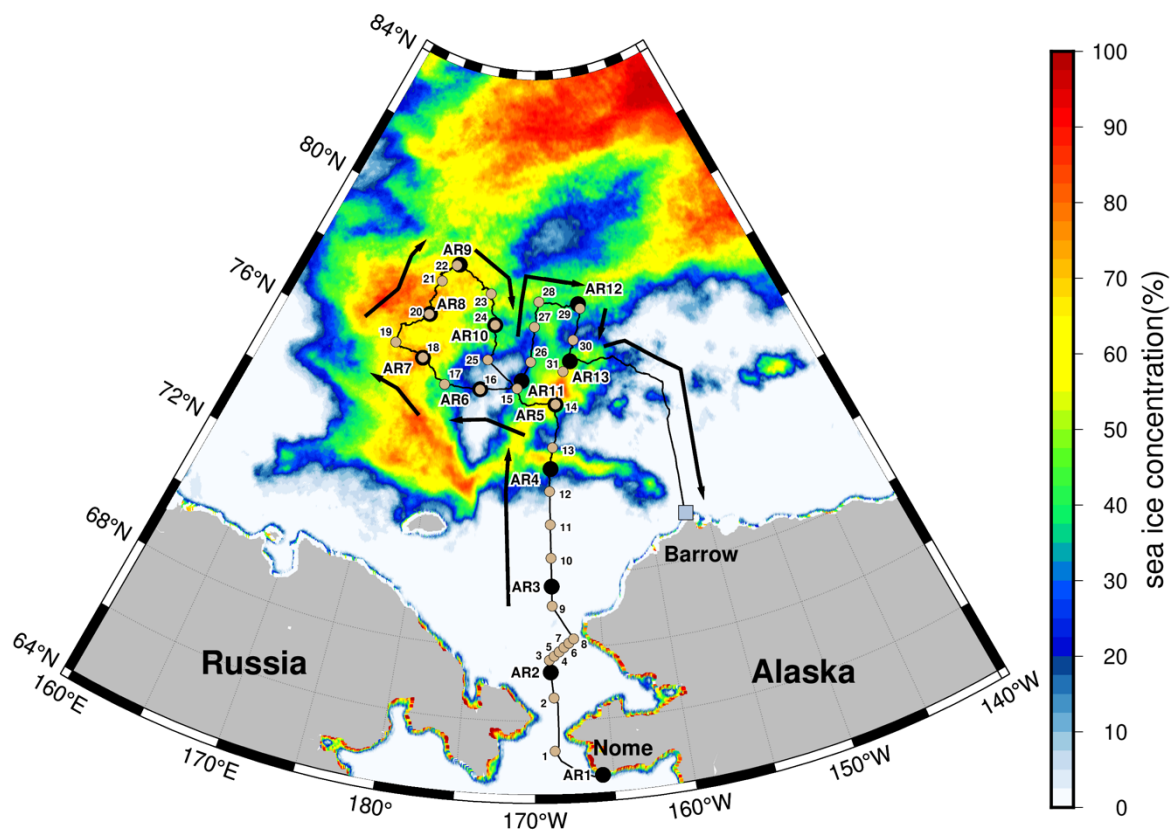
Figure 1: Cruise track (thin black lines) of ARA07B with aerosol (black circles; sample ID: AR1−AR13) and seawater sampling (light brown circles; sample ID: 1−31) locations. Sampling stations were superimposed onto the mean sea ice concentration derived from Advanced Microwave Scanning Radiometer (AMSR) 2 data for August 2016 (Spreen et al., 2008). Each aerosol sampling start point represents the end of the previous sampling period. Black thick arrows indicate the moving direction of the ship.
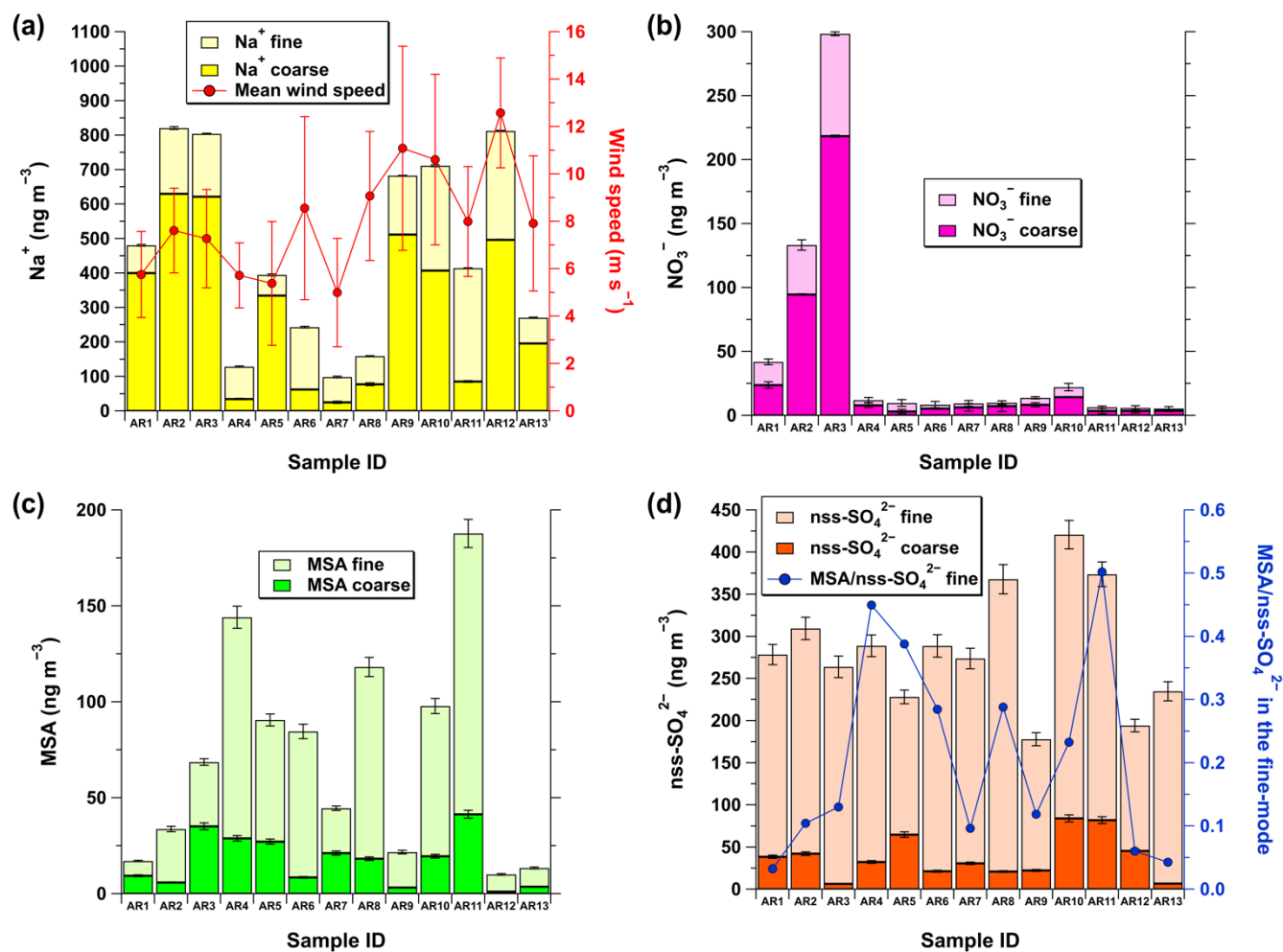
850

Figure 2: Concentrations of (a) Na⁺ (ng m⁻³), (b) NO₃⁻ (ng m⁻³), (c) MSA (ng m⁻³), and (d) nss-SO₄²⁻ (ng m⁻³) in aerosols collected over the western Arctic Ocean during the summer of 2016. The solid red line with circles and error bars in (a) indicates the mean and standard deviation of wind speeds for each aerosol sampling time. The solid blue line with circles in (d) represents the MSA to nss-SO₄²⁻ ratio in the fine-mode aerosols.

855

860
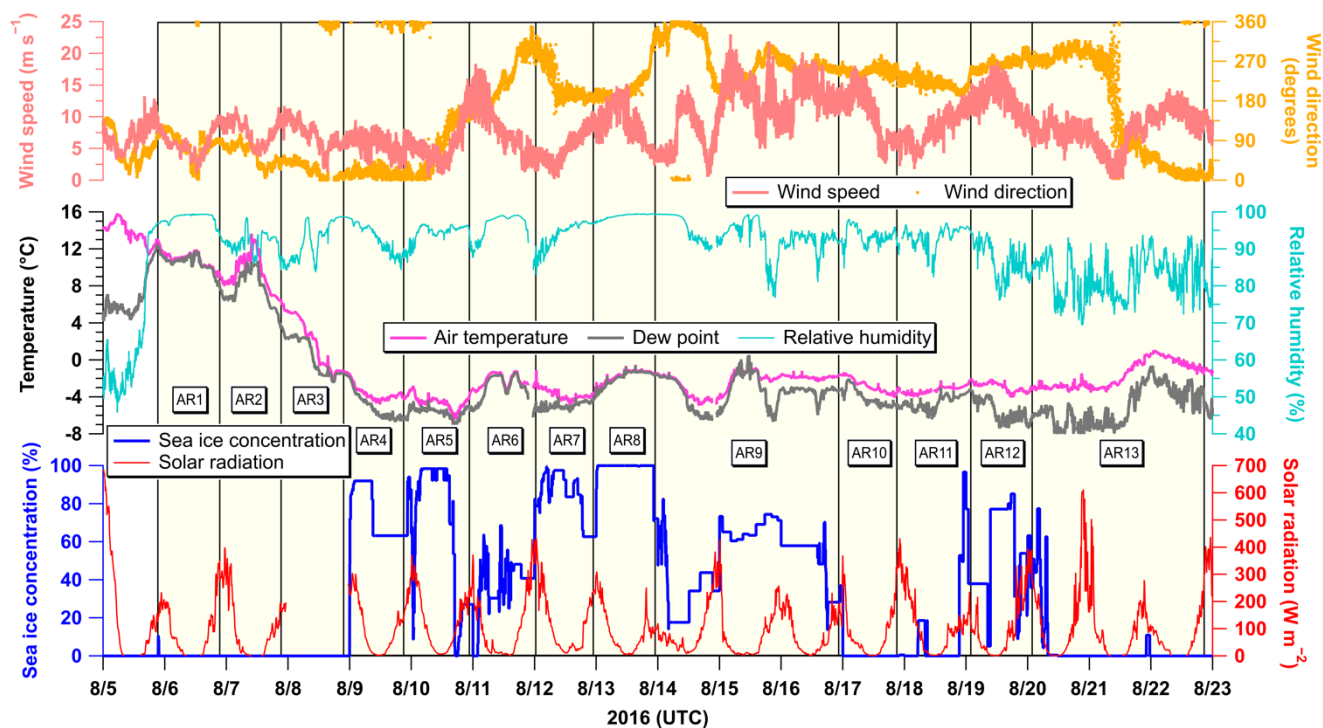
Figure 3: Temporal variations of meteorological variables, including wind speed (m s^{-1}), wind direction (degrees), air temperature (°C), dew point (°C), relative humidity (%), solar radiation (W m^{-2}), and sea ice concentration (%) along the ship's track during the cruise. The yellow hatched area indicates the sampling duration of each aerosol sample (AR1−AR13). Solar radiation was not recorded from 23:20 on 7 August to 23:10 on 8 August due to equipment malfunction. Sea ice concentration represents the percentage of an area covered with sea ice in the ship's location within a 3.125 km × 3.125 km grid derived from AMSR 2 sea ice concentration daily data (Spreen et al., 2008).
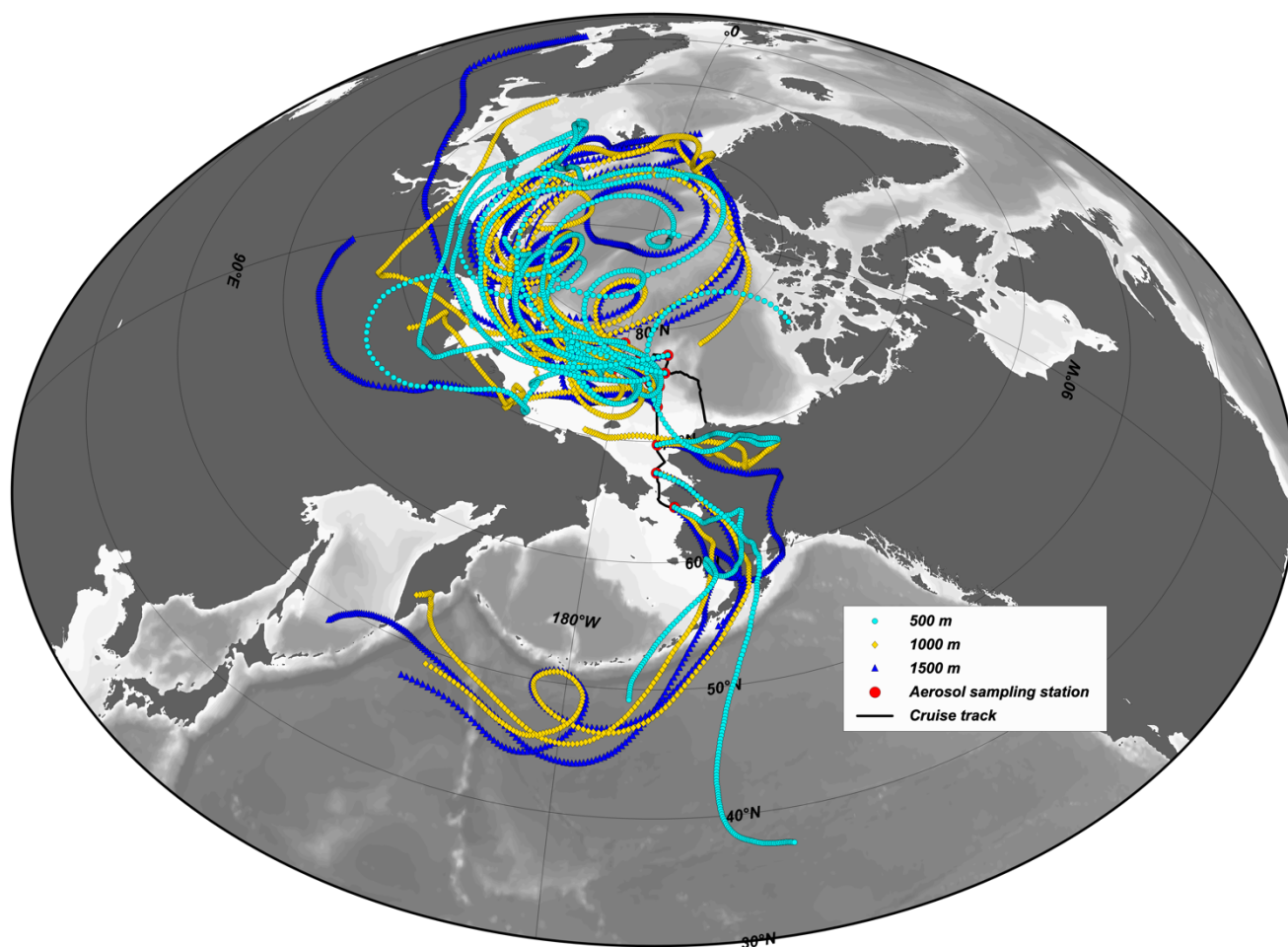
Figure 4: Seven-day backward air mass trajectories at 500 (cyan circles), 1000 (yellow diamonds), and 1500 m (blue triangles) above
885 **ground level for each aerosol sampling station during the cruise. The trajectories were calculated from the GDAS database of the**
NOAA and simulated using the HY-SPLIT model (http:// www.ready.noaa.gov/HYSPLIT_traj.php) (Stein et al., 2015).

890
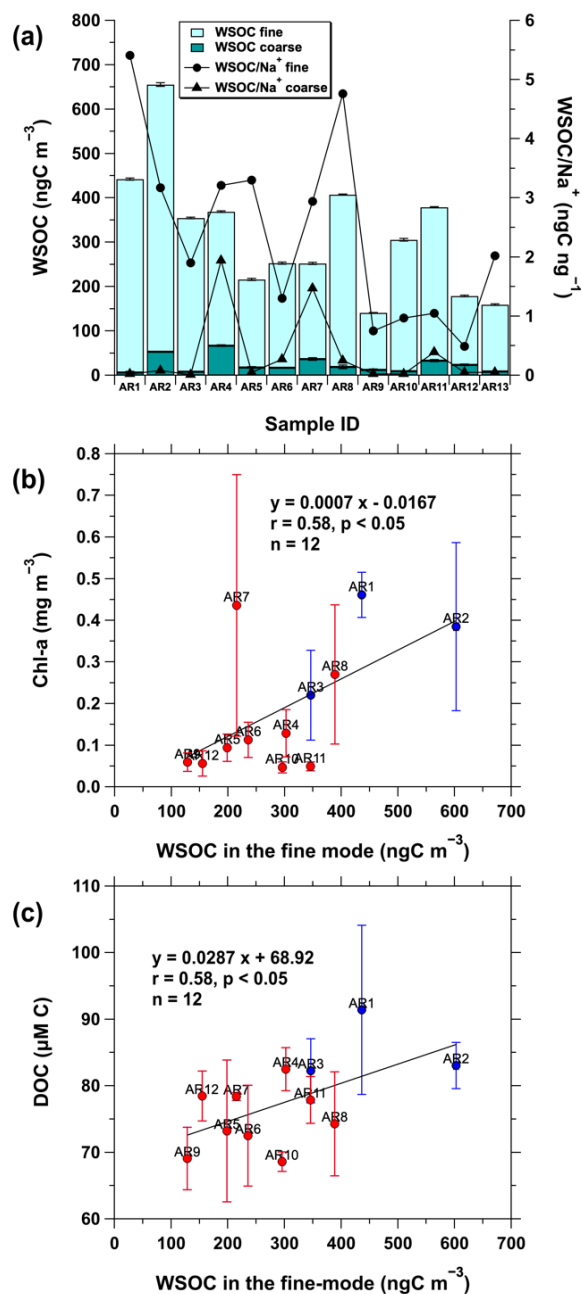
Figure 5: (a) Concentration of WSOC (ngC m^{-3}) and WSOC/Na$^+$ ratio (ngC ng^{-1}) in both fine- (D < 2.5 µm) and coarse-modes aerosols (2.5 µm < D < 10 µm). Relationships of WSOC concentration in the fine-mode aerosols (ngC m^{-3}) with (b) in situ surface chlorophyll-a (Chl-a) concentration (mg m^{-3}) and (c) surface dissolved organic carbon (DOC) concentration (uM C). Chl-a and DOC concentrations are presented in their mean values and standard deviations for each aerosol sampling time. The blue and red solid circles in (b) and (c) indicate the samples collected from the coastal and sea ice-covered areas, respectively. Chl-a and DOC concentrations were not measured during the collection of the AR13 aerosol sample.

895
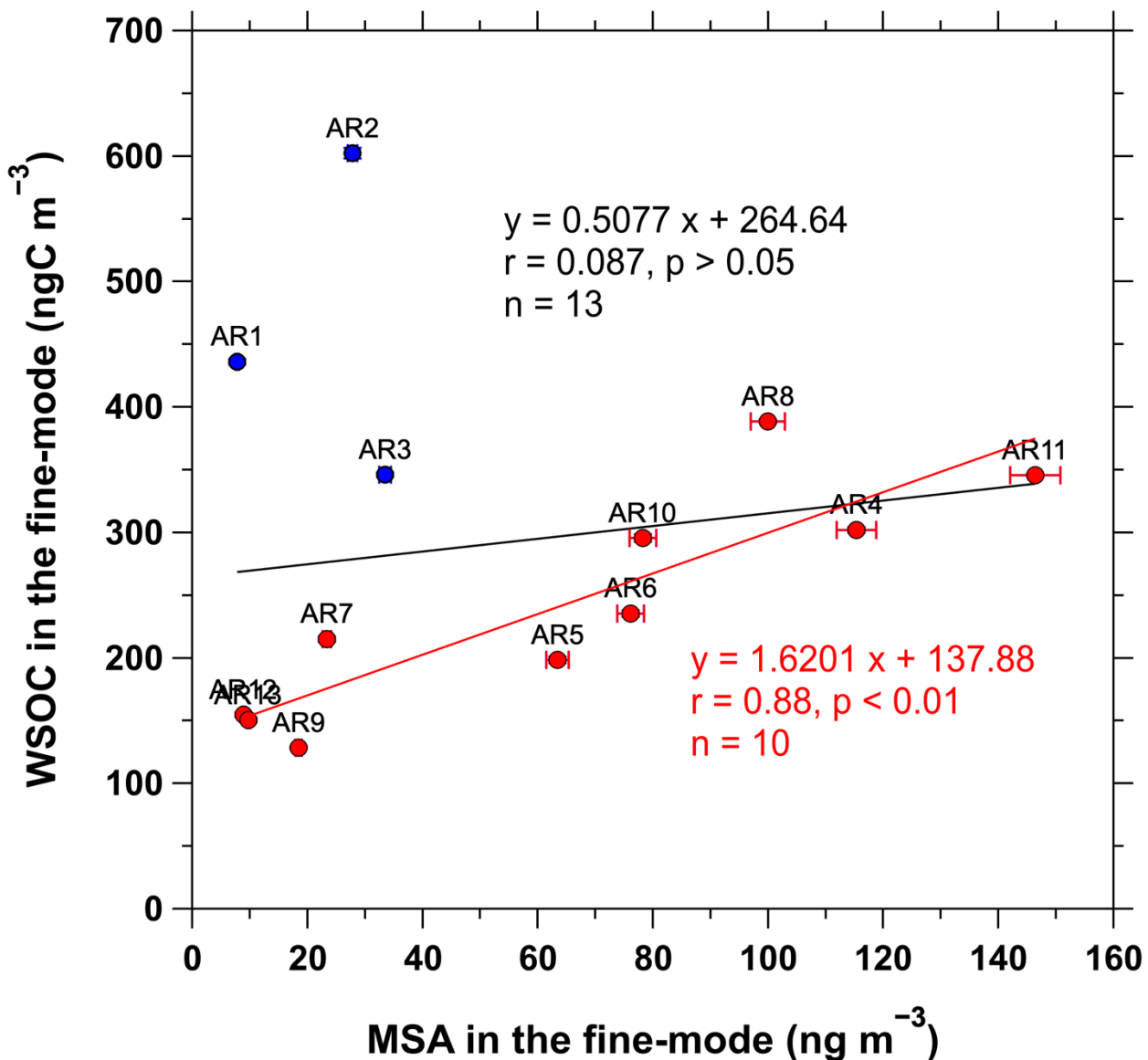
Figure 6: Relationship between WSOC (ngC m⁻³) and MSA (ng m⁻³) in the fine-mode aerosols (D < 2.5 µm) collected during the cruise. The blue and red solid circles indicate the samples collected from the coastal and sea ice-covered areas, respectively. The black and red lines indicate the correlations between WSOC and MSA for the all samples collected during the cruise and for the aerosol samples collected in the sea ice-covered areas of the western Arctic Ocean, respectively.
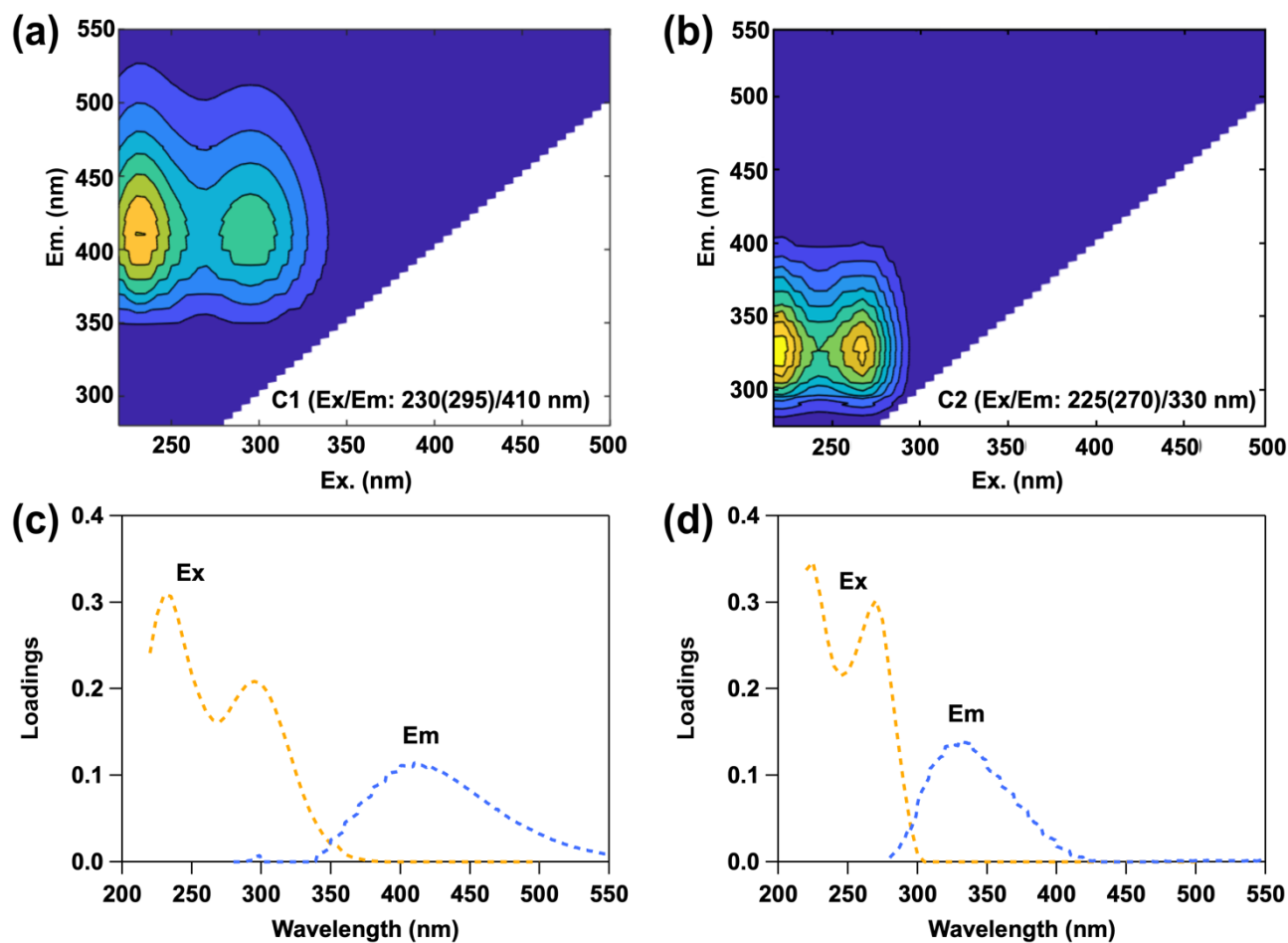
Figure 7: (a and b) Fluorescence EEM contour plots of the two fluorescent components C1 and C2 identified using EEM−PARAFAC in the fine-mode aerosols collected over the western Arctic Ocean during the summer of 2016. (c) and (d) show the excitation and emission spectra of C1 and C2, respectively.

905
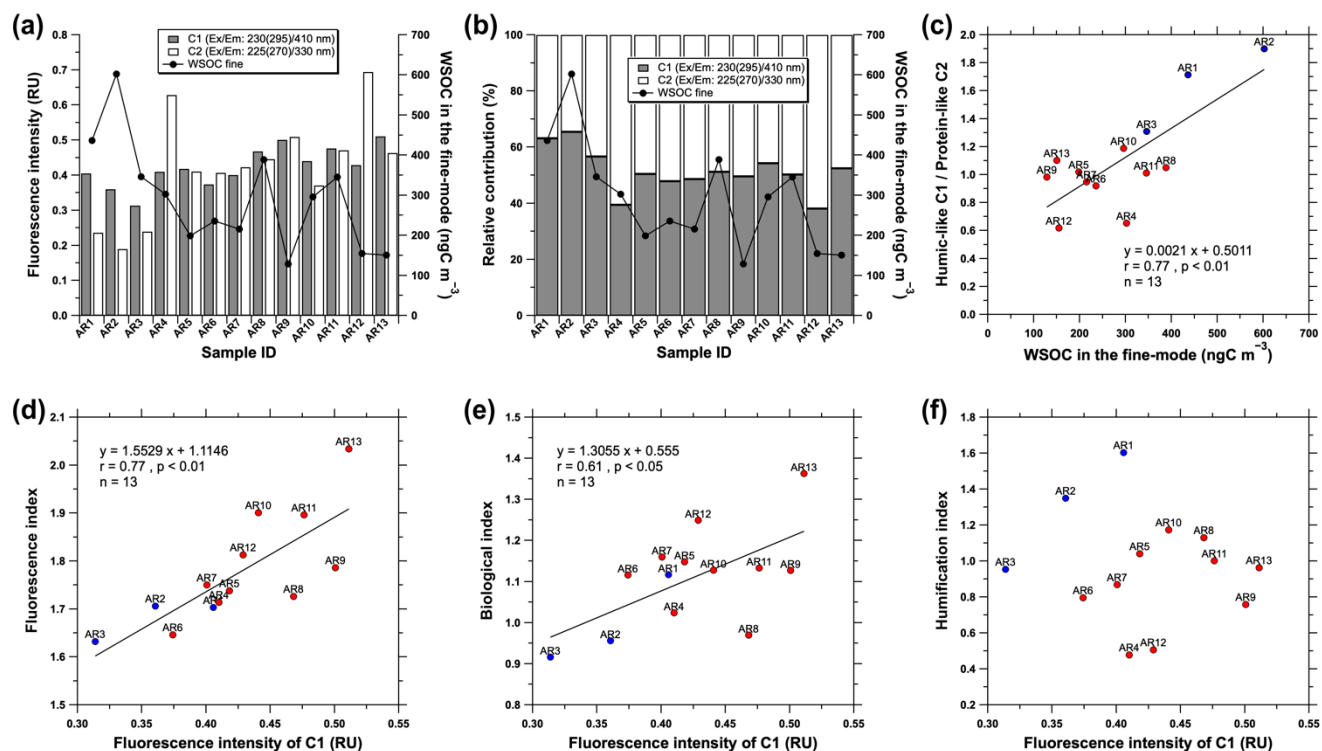
910 **Figure 8: (a) Variations in the fluorescence intensities and (b) relative contributions of C1 and C2 in the fine-mode aerosols collected over the western Arctic Ocean during the summer of 2016. The black lines with circles in (a) and (b) indicate the WSOC concentration in the fine-mode aerosols. (c) Relationship between the fluorescence intensity ratio of the humic-like C1/protein-like C2 and the WSOC concentration in the fine-mode aerosol particles. (d) Fluorescence index (FI), (e) biological index (BIX), and (f) humification index (HIX) as a function of the fluorescence intensity of the humic-like C1 in the fine-mode aerosols. The blue and red**

915 **solid circles in (c)−(f) indicate the samples collected from the coastal and sea ice-covered areas, respectively.**
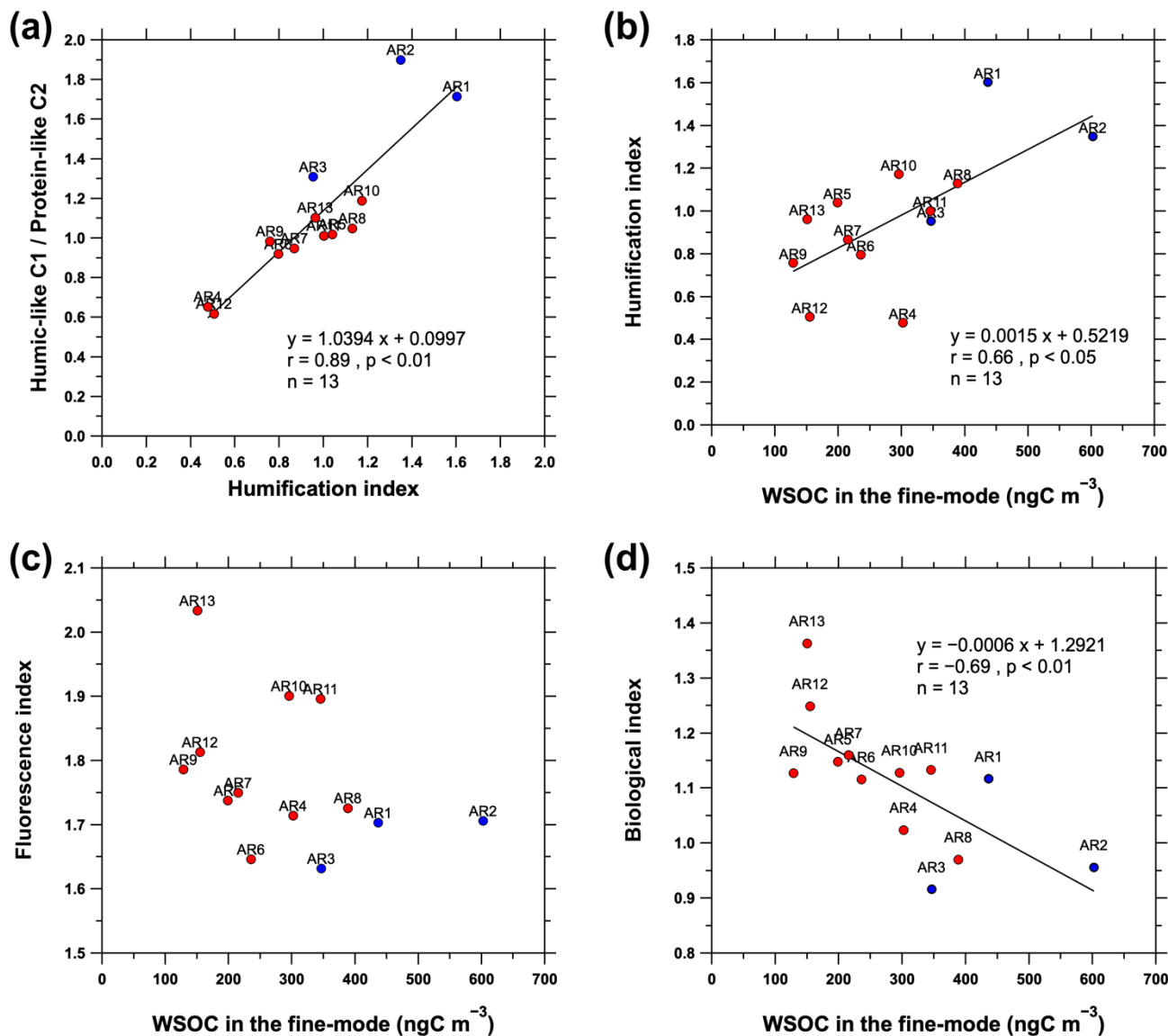
Figure 9: (a) Relationship between the fluorescence intensity ratio of the humic-like C1/protein-like C2 with humification index **(HIX).** Relationships between WSOC concentration in the fine-mode aerosols and **(b)** HIX, **(c)** fluorescence index (FI), and **(d)** biological index (BIX). The blue and red solid circles indicate the samples collected from the coastal and sea ice-covered areas, respectively.